A brain-specific isoform of mitochondrial Apoptosis Inducing Factor: AIF2

Emilie Hangen, Daniela De Zio, Matteo Bordi, Changlian Zhu, Philippe Dessen, Fanny Caffin, Sylvie Lachkar, Jean-Luc Perfettini, Vladimir Lazar, Jean Benard, et al.

CDD-09-0430
Revision date: **Nov. 10, 2009**
Author: Guido Kroemer

POINT-BY-POINT REPLY TO REFEREE NO. 1

The reviewer formulated a series of major concerns

Major point 1 raised by reviewer 1: *Little data are presented concerning the function of AIF2. Does AIF2 fulfill redox function in normal cells, similarly to AIF1? Does AIF2 play a role in cell death?*

Our response: We have addressed the question as to whether AIF2 is as efficient as AIF1 in restoring the function of complex 1 in AIF-deficient cells. The results of these experiments are shown in Figure 6d. It should be noted that the respiratory and redox functions of AIF are closely linked because redox-deficient AIF mutants are unable to restore the abundance and function of respiratory chain complex I from AIF knockout cell (Urbano, A. et al. (2005) EMBO J. 24, 2815–2826), as we have discussed in the text page 10, lines 15 to 20. As a result, it appears that AIF2 has a normal redox function, similar to that of AIF1. As to the second question formulated by the reviewer ("*Does AIF2 play a role in cell death?*"), we are confronted with the problem that none of the cell lines that we characterized predominantly expressed AIF2 (although, based on the in situ hybridization studies, a sizeable fraction of primary brain cells solely express AIF2, not AIF1). Therefore, we cannot address the reviewer's excellent question experimentally at this point, and we have to wait for the results of the knockout experiments in which exon 2b (which is specific for AIF2) has been flanked by lox sites and will be excised enzymatically by tissue-specific expression of the Cre recombinase. Although we have managed to generate mice expressing a floxed exon 2b, it will take us at least six months to generate tissue-specific (and in particular brain-specific) AIF2 knockout mice and to characterize their propensity to cell death. Therefore, it is impossible to furnish clearcut results on the putative pro- or anti-apoptotic functions of AIF2 within the rigid time frame established by CDD (which asks us to resubmit our paper within four months).

Major point 2 raised by reviewer 1: *The authors propose that AIF2 is retained in mitochondria to minimize its neurotoxic effects. Therefore, it would be interesting to compare the oxidation of NAD(P)H by AIF1 versus AIF2. Since AIF2 retains in mitochondria, this critical experiment could reveal whether AIF2 is more important for fulfilling the redox function rather than cell death. Measurement of cell death in the presence or absence of AIF2 (by using the siRNA against AIFexon2a) would also answer this question.*

Our response: We have knocked down AIF2 using a siRNA in SHSY-5Y neuroblastoma cells that express both AIF1 and AIF2, and we have found that this manipulation did not affect the baseline NAD(P)H levels, as determined by assessing the autofluorescence of cells. In line with the report published by Churbanova *et al.* (Redox-dependent changes in molecular properties of mitochondrial apoptosis-inducing factor. *J Biol Chem* 2008; 283: 5622-5631)**,** showing that the NAD(P)H oxidase activity of AIF is very low, our observation suggests that AIF may serve in a local redox signaling function that is yet to be determined. These data have been included in the paper, following the reviewer's suggestion (supplemental Figure 3) and have been commented on in the text (page 10, lines 21 to 23; page 11, lines 1 to 3).

Major point 3 raised by reviewer 1: *Fig. 5d. After expression of AIF 3'UTR siRNA an additional band (the size lower than endo-AIF) is appeared. What is the source of this band?*

Our response: These experiments have been repeated several times, leading to the conclusion that the additional band results from the overexposure of the autoradiographic film. We have replaced the figure accordingly and in the revised manuscript Fig. 5d is now Fig.6d

Major point 4 raised by reviewer 1: *Amount of VDAC in all transfected cells after treatment with detergent is increasing in both pellet and supernatant (Fig. 7a). How it is possible?*

Our response: Driven by the reviewer's constructive critique, we have repeated the VDAC immunoblot detection in conditions in which the amount of cell lysate (antigen) and also the concentration of the secondary antibody were rigorously standardized (Fig. 7A). We suspect that the result that perturbed the reviewer was due to the overexposure of the membrane (which can lead to the paradoxical reduction in the intensity of band, in particular in the center of the band, that corresponds to particularly high concentrations of the antigen+antibody complex detected with the ECL chemoluminescence reagent). This is well known phenomenon (cf. ECL manual).

Major point 5 raised by reviewer 1: *Since AIF2 is specific for neuronal tissues and neuroblastomas, it will be interesting to know whether this protein is also expressing in tumors of neuro-endocrine origin.*

Our response: We enthusiastically welcome the reviewer's suggestion that we will address in forthcoming papers. As it stands, adrenal tissues (which are largely of neuro-endocrine origin) do not express AIF2. Similarly, several melanoma cell lines (which are often deemed to be of neuro-endocrine origin) were negative for AIF2 expression. Therefore, we estimate that it is improbable that AIF2 is expressed in neuro-endocrine tumors. However, this assumption has to be subjected to a thorough verification.

In addition, the reviewer raised two minor critiques:

Minor point 1 raised by reviewer 1: *Fig 2a. Expression of AIF in brain is unexpectedly lower in comparison to liver and heart keeping in mind the importance of AIF-mediated cell death for neuronal cells. This should be discussed. Is the expression level low to reduce toxicity? Or might it be so that the redox function/capacity of AIF in brain is not so important as compared to in liver, heart, etc?*

Our response: Following the reviewer's recommendations, we have discussed the comparatively low AIF expression in brain as compared to liver and heart in the Results (page 8, lines 4 to 8). In a report published by Benit et al. (*PLoS ONE* 2008; **3**: e3208), the amount of AIF protein in various murine organs was compared to that of another mitochondrial protein (VDAC/porin) and it was found that in all analyzed organs (cerebellum, spinal cord, cortex, retinas, heart, skeletal muscle, kidney and liver) the ratio AIF/VDAC was similar. In conclusion, these published data indicate that a low level of AIF, in brain compared to heart or other organs, is a sign of a lower amount of total mitochondrial proteins.

Minor point 2 raised by reviewer 1: *Page 7. What does mean: "the two exons were generated by gene duplication well before the mammalian radiation"?*

Our response: The criticized phrase on page 7 (lines 5 to 9) has been reformulated.

“Likewise, the two exons were generated by gene duplication well before the speciation of mammals (data not shown). Indeed, we were able to trace the duplication event to chicken genome, where a region homologous to the mammalian exon 2a can be found 5' of exon 2b on chromosome 4, although the splice acceptor site of exon 2a seems to be non canonical (UCSC, genome browser).”

POINT-BY-POINT REPLY TO REFEREE NO. 2

The reviewer formulated a series of specific points of critique:

Specific point 1 raised by reviewer 2: *AIF has to be cleaved from its membrane anchor, the transmembrane segment partially encoded in the alternative exons, before it can be released from mitochondria. The cleavage site however appears to be located in the intermembrane space, hence this region is similar between AIF1 and AIF2. This suggests that cleavage should occur independently of the matrix located isoform specific N-terminal regions. A model in which the different hydrophobicities could account for different efficiencies to release AIF does not make sense in the light of many data on the requirement of processing of AIF prior to its release from mitochondria (e.g. Polster et al. 2005, Otera et al. 2005,…).*

Our response: We have carefully considered this point raised by the reviewer. Although the reviewer is, in principal, correct in her/his affirmation, it appears that AIF2 is more difficult to be released from mitochondria than AIF1. Therefore, it appears that the mitochondrial release-associated cleavage of AIF2 is more difficult to be achieved than AIF1. This difference cannot be explained by differences in the primary sequence of the cleavage site. Rather, they must be linked to other properties of the molecule such as the accessibility of AIF2 (which may be more profoundly "buried" in its N-terminus in the lipid bilayer of the inner mitochondrial membrane than AIF1). In support of this possibility, we would like to mention that biochemical studies of AIF1 carried out by Churbanova et al. (Redox-dependent changes in molecular properties of mitochondrial apoptosis-inducing factor. *J Biol Chem* 2008; 283: 5622-5631) suggest that redox-regulated changes in the conformation of AIF that implicate its N-terminal and C-terminal segments might determine the dimerization of AIF, its accessibility to apoptotic proteases and by consequence its mitochondrial release in dying cells. This point has been explicitly expressed in the revised version of the manuscript (page 12, lines17 to 23; page 13, lines 1 to 3).

Specific point 2 raised by reviewer 2:. *Experiment 7c: It is essential to show at least two fractions of this fractionation including the membrane (hence mitochondria containing) fraction. As the figure is now, it is impossible to judge whether the differences in AIF release stem from different expression levels (even of the normal AIF, as Figure 7b would suggest lower level of AIF if AIF2-FLAG is overexpressed), or whether the non released AIF is found in the pellet, or whether part of the AIF is found in another localization (e.g. the nucleus).*

Our response: We have repeated the experiment shown in Fig. 7c, including the additional control requested by the reviewer. This improved experiment is now fully included in the revised version of

the paper. As an additional control, we checked the release of another mitochondrial protein (EndoG), whose release was not affected by AIF1 or AIF2. As the reviewer will appreciate, there is a clear difference in the mitochondrial release of AIF1 versus AIF2. We thank the reviewer for her/his elegant suggestion that helped to improve our paper.

Specific point 3 raised by reviewer 2: *Experiment 7d lacks controls (i.e. non precipitated control proteins).*

Our response: In accord with the reviewer's suggestion, the whole cell lysate controls (Input) were clearly indicated in Fig. 7d.

Specific point 4 raised by reviewer 2: *It would be desirable to use one cellular model in a consistent way for the cell biology part of the manuscript to allow the transfer of the different sets of data (EM in U20S cells versus fractionation with HeLa cells).*

Our response: To streamline the data representation and to focus on essential facets of the paper, the electron microscopy results obtained on stably transfected U2OS were moved to the supplementary Fig. 4. This figure contains additional data obtained with the same cell line that overexpress either AIF1 or AIF2.

Specific point 5 raised by reviewer 2:. *Figure legend 7b: Na-bicarbonate should be Na-carbonate.*

Our response: This error has been corrected.

Specific point 6 raised by reviewer 2: *6. Can AIF2 be cleaved to the same extent by calpains and cathepsins as AIF1?*

Our response: We have attempted to generate recombinant full-length AIF1 and AIF2 (with the entire N-terminus) and thus far have failed to obtain a correctly folded protein. As a result, we have been unable to perform the requested proteolytical experiments. However, we feel the proteolysis of purified proteins may not reflect that of their membrane-embedded equivalents. We have discussed the proteolytic cleavage of AIF in the revised paper (page 12, lines17 to 23; page 13, lines 1 to 3).

Specific point 7 raised by reviewer 2:. *Why has expression of AIF2 a dominant negative effect on cristae formation and AIF accumulation (and possibly release)?*

Our response: We have no explanation on how AIF might affect cristae formation (although AIF might of course, theoretically, affect membrane curvature). As it stands, we simply report that ovexpressed AIF1 and overexpressed AIF2 affect the morphology of mitochondria in a clearly distinguishable fashion, pointing to differences between AIF1 and AIF2 (perhaps because both proteins impose different levels of membrane curvature). Since these data are based on the transfection-enforced overexpression of both isoforms, they can be criticized and have been moved to the supplemental section of the paper. However, we have provided a hypothetical explanation how AIF2 may inhibit the release of AIF1, namely by forming heterodimers (or perhaps higher-order hetero-oligomers). In this case, the more membrane-anchored isoform would retain the more "voluble" isoform in mitochondria, as we have discussed in the revised version of the paper (page 12, lines17 to 23; page 13, lines 1 to 8).

POINT-BY-POINT REPLY TO REFEREE NO. 3

The reviewer formulated one single point of critique: *In this manuscript Authors perform a thorough characterization of AIF2, showing that it is specifically expressed in neurons and more tightly anchored to the inner mitochondrial membrane. The data are convincing and solid. However, what is really missing from the paper to be a strong candidate for CDD are the cell death experiments. If the Authors had an experiment of selective silencing of AIF2 in neurons, or of both forms with the reintroduction of a resistant AIF2 variant and then they tested the impact on neuronal viability/function/cell death the paper would be perfect. As it is, I see it more suited for a Journal where to report the characterization of a novel splice variant of an important gene, like JBC, or a neurobiology Journal.*

Our response: The reviewer criticized the absence of cell death experiments from our paper and insinuates that this would be sufficient to question the suitability of our paper for CDD. "Cell Death & Differentiation" has a dual scope. The journal deals with cell death mechanisms, as well as will mechanisms of cell differentiation. In our paper, we show that AIF is expressed in a differentiation-dependent fashion in the developing brain of mice and humans. We show that AIF is specifically expressed in the brain in some particular cell types. Moreover, we show that AIF1 and AIF2 differ in their propensity to be released from mitochondria by a series of pharmacological and chemical inducers. Therefore, we believe that our paper qualifies for publication in CDD (placing emphasis on the second, not the first, "D"). The reviewer requested experiments in which we would silence AIF2 in cells that express AIF2. These experiments have also been asked for by reviewer 1 (see points 1 and 2 raised by this referee), and new data have been added to the paper.

As we have explained in our point-by-point reply to reviewer 1, we are confronted with the problem that none of the human or murine cell lines that we characterized thus far predominantly expressed AIF2 (although, based on the in situ hybridization studies, a sizeable fraction of primary brain cells solely express AIF2, not AIF1). Therefore, we have to wait for the results of the knockout experiments in which exon 2b (which is specific for AIF2) has been flanked by lox sites and will be removed by tissue-specific expression of the Cre recombinase. Although we have been successful in generating mice expressing a floxed exon 2b, we will need more than six months to generate tissue-specific (and in particular brain-specific) AIF2 knockout mice and to characterize their susceptibility to cell death. Therefore, we are unable to furnish results on the putative pro- or anti-apoptotic functions of AIF2 within the calendar established by the Nature Publishing Group for resubmission.

To meet the reviewer's critique, we have included additional data that show that AIF2 is upregulated in human mesencephalic neural progenitor cells as they differentiate *in vitro* into post-mitotic dopaminergic neurons. Our results clearly indicate that the expression level of AIF2 depends on the differentiation status of neuronal cells, both in the human and in the mouse systems. This finding suggests that our paper is optimally suitable for publication in CDD.

END

A brain-specific isoform of mitochondrial Apoptosis Inducing Factor: AIF2

Emilie Hangen[1,2,3], Daniela De Zio[4,5], Matteo Bordi[4,5], Changlian Zhu[6], Philippe Dessen [2,3,7], Fanny Caffin[1,2,3], Sylvie Lachkar[1,2,3], Jean-Luc Perfettini[1,2,3], Vladimir Lazar[2,3,8], Jean Benard[2,3,9], Gian Maria Fimia[10], Mauro Piacentini[10], Francis Harper[11], Gérard Pierron[11], José Miguel Vicencio[1,2,3], Paule Bénit[12,13,14], Anderson de Andrade[16], Günter Höglinger[16], Carsten Culmsee[17], Pierre Rustin[12,13,14], Klas Blomgren[6,15], Francesco Cecconi[4,5], Guido Kroemer[1,2,3*#] and Nazanine Modjtahedi[1,2,3*#]

[1]INSERM U848; [2]Institut Gustave Roussy, Villejuif-France; [3]University Paris 11-France; [4]Dulbecco Telethon Institute at the Department of Biology, University of Rome 'Tor Vergata', 00133 Rome, Italy; [5]Laboratory of Molecular Neuroembryology, IRCCS Fondazione Santa Lucia, 00143 Rome, Italy; [6] Center for Brain Repair and Rehabilitation, Institute of Neuroscience and Physiology, University of Gothenburg, Gothenburg, Sweden; [7]CNRS FRE2939, [8]Functional genomic Unit, [9]CNRS UMR8126, [10]National Institute for Infectious Diseases "Lazzaro Spallanzani", 00149 Rome, Italy ; [11]Laboratoire "Réplication de l'ADN et Ultrastructure du Noyau" CNRS-Institut André Lwoff- 94801 Villejuif- France [12,] INSERM U676 ; [13]Hôpital Robert Debré, Paris-France ; [14]University René Diderot, Paris-France; [15]Department of Pediatric Oncology, Queen Silvia Children's Hospital, Gothenburg, Sweden; [16]Experimental Neurology, Philipps University, Marburg, Germany ; [17]Institute for Pharmacology und Toxicology, department of Pharmacy, Philipps-University Marburg.

#These authors share co-senior authorship.

*Correspondence:

Guido Kroemer
INSERM, U848
Institut Gustave Roussy
Pavillon de Recherche 1
F-94805 Villejuif (Paris)-France
Tel. +33 1 42 11 60 46
Fax. +33 1 42 11 60 47
kroemer@orange.fr

Nazanine Modjtahedi
INSERM, U848
Institut Gustave Roussy
Pavillon de Recherche 1
F-94805 Villejuif (Paris)-France
Tel. +33 1 42 11 54 91
Fax. +33 1 42 11 66 65
nazanine@igr.fr

Running title: Brain-specific AIF2

Key Words: brain development, neural differentiation, neural progenitor, neuroblastoma,

oxidative phosphorylation

Abbreviations: CNS: central nervous sytem; FISH: fluorescent in situ hybridization; LUHMES: Lund Human Mesencephalic neurons; IMSS: inner membrane sorting signal; MLS: mitochondrial localization signal; MOMP: mitochondrial outer membrane permeabilization. NCI: National Cancer Institute; NLS: nuclear localization signal; TEM: transmission electron microscopy.

Abstract

Apoptosis-Inducing factor (AIF) plays important supportive as well as potentially lethal roles in neurons. Under normal physiological conditions, AIF is a vital redox-active mitochondrial enzyme, whereas in pathological situations, it translocates from mitochondria to the nuclei of injured neurons and mediates apoptotic chromatin condensation and cell death. Here, we reveal the existence of a brain-specific isoform of AIF, AIF2, whose expression increases as neuronal precursor cells differentiate. AIF2 arises from the utilization of the alternative exon 2b, yet uses the same remaining 15 exons as the ubiquitous AIF1 isoform. AIF1 and AIF2 are similarly imported to mitochondria where they anchor to the inner membrane facing the intermembrane space. However, the mitochondrial inner membrane sorting signal (IMSS) encoded in the exon 2b of AIF2 is more hydrophobic than that of AIF1, indicating a stronger membrane anchorage of AIF2 than AIF1. AIF2 is more difficult to be desorbed from mitochondria than AIF1 upon exposure to non-ionic detergents or basic pH. Furthermore, AIF2 dimerizes with AIF1, thereby preventing its release from mitochondria. Conversely, it is conceivable that a neuron-specific AIF isoform, AIF2, may have been "designed" to be retained in mitochondria and to minimize its potential neurotoxic activity.

Introduction

Apoptosis-inducing factor (AIF) has initially been described as a mitochondrial intermembrane protein that is released from mitochondria under conditions of cell death induction and that can induce isolated nuclei to undergo nuclear shrinkage and chromatinolysis, two features that are classically associated with apoptosis.[1] Since its discovery ten years ago, the AIF protein has been characterized at the structural level,[2,3] and the AIF gene has been subjected to genetic manipulations in mice, flies, nematodes and yeast, revealing the phylogenetically conserved contribution of AIF to cell death in multiple systems.[4,5]

After the mitochondrial import of the precursor AIF protein and the removal of its N-terminal 53 amino acids, which includes a mitochondrial localization sequence (MLS), the processed mature human AIF 62-kDa is inserted into the inner mitochondrial membrane, with the N-terminus facing the matrix and with the C-terminal catalytic domain exposed to the intermembrane space.[6] The mitochondrial AIF protein is an NAD(P)H oxidase[7] whose local redox function is essential for optimal oxidative phosphorylation.[8] Knockdown, deletion or hypomorphic mutation of *AIF* (the *harlequin* or *Hq* mutation) reduces the expression of complex I subunits in the respiratory chain,[8] thereby provoking a mitochondriopathy that leads to progressive neurodegeneration, photoreceptor loss and cardiomyopathy.[9-13] The consistent finding that the targeting of AIF mostly affects the central nervous system (CNS)[9] might either be explained by the general tendency of complex I mitochondriopathies to manifest at the level of the CNS[14] and/or by an implication of AIF in the differentiation of neuronal cell precursors.[12]

Upon apoptotic stimuli, AIF, which is able to directly interact with DNA,[15] translocates to the nucleus and participates in chromatin condensation and chromatinolysis.[16] The switch from the vital to the lethal functions of AIF is spatially regulated by its subcellular localization and tightly controlled by at least two processes: (i) outer mitochondrial membrane permeabilization (MOMP), which is regulated by multiple mitochondrial proteins including members of the Bcl-2 family,[17] (ii) activation of a series of non-caspase cysteine proteases (including calpains and cathepsins) that cleave the N-terminal membrane insertion domain at amino acid 101, thus catalyzing the de-attachment of mature AIF from the inner mitochondrial membrane.[5,6,18]The nuclear translocation of AIF could be inhibited by the overexpression of heat shock protein 70, which can intercept AIF in the cytosol[19] or deletion of cyclophilin A, which is required for AIF to move into the nucleus.[20] In mice, the *Hq* mutation has been shown to reduce acute neuronal cell death after ischemia, hypoglycemia and neurotrauma in young animals, before they manifest the *Hq*-associated neurodegeneration.[21] However, the *Hq* mutation had no cardioprotective effect[13] and was not able to make islet beta cells more resistant to hydrogen peroxide-induced cell death,[22] suggesting that AIF contributes to lethal signaling in a cell type-specific fashion.

Through alternative splicing, the precursor mRNA transcribed from the AIF gene can give rise to several distinct proteins. Thus, alternative utilization of the exons 2a or 2b of the AIF gene (16 exons in total) gives rise to AIF1 (the originally described isoform of AIF) or AIF2 (which has been found in cDNA libraries from fetal mouse tissues), respectively. AIF1 and AIF2 only differ in a short stretch of their amino acid sequence in the N-terminal region that is removed from the mature protein as it translocates to the nucleus.[23] Numerous functional studies have been performed on AIF1, the most abundant and ubiquitous AIF isoform, whereas, AIF2 has not been further characterized. In addition to the above-mentioned isoforms, an alternate transcriptional

start site located at intron 9 of AIF originates a short variant of the protein (AIFsh) that lacks the N-terminal MLS and the redox-active domain, yet retains the nuclear localization sequence (NLS). The transfection-enforced overexpression of AIFsh results in a nuclear protein that causes apoptosis.[24] Moreover, another short form of AIF, AIFsh2, results from the alternative utilization of exon 9b (instead of 9), which contains a stop codon. AIFsh2 is a truncated protein that lacks the C-terminal pro-apoptotic domain, yet conserves its mitochondrial localization and redox function.[25] Both short AIF isoforms appear to be low-abundant in normal tissues because they have not been detected by immunoblot, with the exception of AIFsh2 that reportedly is present in liver extracts.[24,25]

By characterizing the tissue expression profile of AIF isoforms, we discovered that AIF2 is specifically expressed in the CNS. Driven by the pathophysiological impact of AIF in neurodegeneration,[9,11,12] we performed an exhaustive functional and biochemical characterization of the AIF2 isoform and importantly, we found that, compared to AIF1, AIF2 possess a stronger anchoring capacity to the inner mitochondrial membrane. These results suggest that the neuron-specific AIF2 isoform has been "designed" for maintaining its mitochondrial functions yet reducing its pro-apoptotic activities.

Results and Discussion

A novel brain-specific isoform of AIF, AIF2. When sequencing several cDNAs from fetal human brain, we detected an alternative exon2 usage (Fig. 1a), indicating that the precursor of the human AIF mRNA can be alternatively spliced, yielding two isoforms that we designated AIF1 (when exon 2a is used) and AIF2 (when exon 2b is used). The alternative exons 2a and 2b are phylogenetically conserved among mammals. Likewise, the two exons were generated by gene duplication well before the speciation of mammals (data not shown). Indeed, we were able to trace the duplication event to chicken genome, where a region homologous to the mammalian exon 2a can be found 5' of exon 2b on chromosome 4, although the splice acceptor site of exon 2a seems to be non canonical (UCSC, genome browser). Thus, both exons 2a and 2b are detectable in published cDNA sequences from primates, rodents and other mammals (such as *Equus caballus* and *Canis familiaris*) (NCBI-Homologen database), whereas only one exon 2, which resembled exon2b from mammals, could be discerned in chicken cDNA libraries (Fig. 1b, c). Amino acid alignments of exons 2a and 2b from several animal species revealed two positively- and one negatively-charged common residues, as well as conserved motifs with hydrophobic stretches (Fig. 1c). However, secondary structure predictions indicate the consequences of variable residues and their differential properties on the potential secondary structure of the segment encoded by each of the two exons (Fig. 1d).

Quantitative expression profiling of the two AIF isoforms showed that *AIF2* mRNA was specifically detected in human brain, yet was absent from most other analyzed tissues except the

retina (Fig. 2a). Within the human adult brain, *AIF2* mRNA was found in all regions, including the cortex or in subcortical areas, and the expression level of *AIF1* and *AIF2* mRNAs were similar (Fig. 2b). This general expression profile was similar for all examined mouse tissues, where *AIF2* mRNA was again restricted to the brain (Fig. 2c). Both in human and mice, low levels of AIF expression were detected in the brain compared to other organs. This probably reflects the comparative paucity of mitochondria in the brain, because the ratio of AIF protein and the most abundant outer mitochondrial membrane protein, VDAC, is similar in a panel of distinct mouse organs including brain[14]. The expression levels of *AIF1*- and *AIF2*-specific mRNAs were equivalent in the adult mouse brain and were similarly affected by the hypomorphic *Hq* mutation that reduced the expression of both *AIF1* and *AIF2* to around 20% of the control level (Fig. 2d). Of note, the expression of human AIF2 mRNA was higher in adult brain than in fetal brain (while that of *AIF1* was lower) (Fig. 2b), indicating that the *AIF1*/*AIF2* ratio decreases as brain cells differentiate. Accordingly, mouse embryonic telencephalic cells immortalized with thermosensitive SV40 large T antigen (tsA58 LT-Ag) (Fig. 3a, b), or human embryonic mesencephalic cells immortalized with a v-Myc retroviral vector (Fig 3c) could be stimulated to express higher AIF2 levels upon *in vitro* differentiation. Thus, AIF2 is specifically and differentially expressed in brain cells, depending on their maturation status.

Next, we determined the relative *AIF1* and *AIF2* mRNA expression in the NCI (National Cancer Institute) panel of cancer cell lines (NCI60). While *AIF1* was expressed by all cells, independently of their tissue origin, *AIF2* was absent from all samples (supplemental Fig. 1), including from brain cancer cell lines, of glial origin, contained in the NCI panel (Fig. 4a). However, *AIF2* was expressed by a fraction of neuroblastomas (Fig. 4a and b), in line with the

data obtained on normal, untransformed tissues (see above, Fig. 2). In conclusion, AIF2 is specific for neuronal tissues and neuroblastomas.

Cellular and subcellular localization of AIF2. Comparative *in situ* hybridizations of the adult mouse brain with isoform-specific probes revealed a similar macroscopic distribution of *AIF1* and *AIF2* mRNAs, with peak intensities in the olfactory bulb, rostral migratory stream, olfactory cortex and pituitary (Fig 5a-f, negative controls with anti-sense probes are shown in Supplemental Fig. 2). To investigate whether both *AIF* isoforms are expressed in the same cells, we performed a simultaneous fluorescent *in situ* hybridization (FISH) with differentially labeled exon 2a- and 2b-specific probes (red and green, respectively). In most brain regions, *AIF1* and *AIF2* were co-expressed by the same cells. However, approximately 25% of the cells present in the anterior olfactory nucleus stained uniquely for the exon 2b-specific probe, indicating the existence of brain cells that solely express *AIF2* (and not *AIF1*) (Fig 5g-i).

AIF1 and AIF2 share an identical N-terminal MLS, while their exon 2-encoded inner membrane-sorting signals (IMSS) differ (Fig 1). In order to investigate whether this difference might affect the mitochondrial localization of AIF2, we compared the subcellular distribution of AIF1 and AIF2 by transfecting Hela cells with Flag-tagged versions of AIF1 or AIF2 (with the Flag fused to the C-terminus). When transfected cells were fixed and permeabilized with paraformaldehyde plus Triton X100 and stained with a Flag-specific antibody (Fig. 6a), we found both proteins similarly redistributed into mitochondria (which were labeled with a matrix-targeted fluorescent protein, dsRed-mito), with no discernible effects on the overall shape of the mitochondrial network. Differential permeabilization of the outer mitochondrial membrane (with 0.4 mg/ml

digitonin) and the inner membrane (with 0.8 mg/ml digitonin) allowed antibodies specific for Tim23 (an inner membrane-anchored protein) and cyclophilin D (a soluble matrix protein), respectively, to access mitochondria (Fig. 6b). In these conditions, a Flag-specific antibody gained access to AIF1 and AIF2 similarly, as soon as the outer mitochondrial membrane was permeabilized (Fig. 6b, c), in concordance with the notion that both proteins expose their flagged C-termini to the intermembrane space.

AIF-deficient cells exhibit reduced abundance of complex I subunits, resulting in a severe respiratory dysfunction.[8] Accordingly, small interfering RNAs specific for exon 2a or the 3'UTR of AIF led to a marked reduction in the expression of the 20 kDa complex I subunit (CI SU20) (Fig. 6d) and other complex I subunits (not shown) in U2OS cells (which only express AIF1). The transfection of *AIF2* (whose expression is not impeded by either of the two siRNAs) blunted the depletion of CI SU20 induced by AIF1 knockdown, as much as did the transfection of *AIF1* (whose overexpression is abolished by the exon 2a-specific siRNA, yet not affected by the 3'UTR-specific siRNA) (Fig. 6d). These results corroborate the hypothesis that both *AIF* isoforms are localized in the same submitochondrial compartment where they both sustain the biogenesis or stability of complex I from the respiratory chain. It should be noted that the respiratory and redox functions of AIF are closely linked because redox-deficient AIF mutants are unable to restore the abundance and function of respiratory chain complex I from AIF knockout cell. [26] Therefore, it appears plausible that AIF2 has a normal redox function, similar to that of AIF1. Recently, Churbanova et al. [27] reported a rather low NAD(P)H oxidase activity for a recombinant AIF protein that resembles endogenous AIF more closely than a His-tagged, truncated protein that had been investigated previously.[7] In line with this possibility, we found

that the siRNA-mediated depletion of AIF1 and/or AIF2 from SHSY-5Y neuroblastoma cells (which express both AIF1 and AIF2) did not affect cellular NAD(P)H levels (Supplemental Fig.3).

Biochemical differences between AIF1 and AIF2. In order to detect further possible differences between AIF1 and AIF2, we stably transfected the Flag-tagged versions of both proteins in U2OS cells, obtaining supraphysiological levels of AIF1 and AIF2 (Supplemental Fig. 4a). Both Flag-tagged *AIF1* and *AIF2* cDNAs led to the expression of proteins with a similar electrophoretic mobility corresponding to ~65 kDa (Supplemental Fig. 4a), and similar co-migration results were obtained for non-tagged versions of AIF1 and AIF2 (not shown). The overexpression of AIF1 or AIF2 had neither deleterious effect on the proliferation rate (not shown), nor affected the respiratory capacity and control of the cells (Supplemental Fig. 4b). However, both AIF isoforms differentially affected the ultrastructure of mitochondria, as detectable by transmission electron microscopy (TEM). AIF1 (but not AIF2) overexpression lead to a rarefaction of cristae, while AIF2 (but not AIF1) overexpression tended to increase the curvature of cristae, which frequently adopted an onion-like shape (Supplemental Fig. 4c). Although this result was obtained in conditions in which the two AIF isoforms were overexpressed, it suggested subtle differences in the impact of the insertion of their putative transmembrane domains on mitochondrial membrane structure.

Driven by these results, we investigated whether AIF1 and AIF2 actually differ in their membrane anchorage, in conditions in which Flag-tagged AIF1 and AIF2 are expressed at physiological levels (lower than endogenous AIF, Fig. 7a,b). AIF1 versus AIF2-expressing cells

were exposed to increasing concentrations of the non-ionic detergent Igepal CA-630, and the extractability of the two AIF isoforms was measured. While Igepal CA-630 efficiently extracted AIF1 from mitochondria, AIF2 was largely resistant to the detergent and remained bound to the ultra-centrifugable pellet. Thus, AIF2 behaves like the inner membrane-anchored CI SU20, while AIF1 behaved like several soluble mitochondrial proteins including cytochrome *c* (Fig. 7a). When, the Igepal CA-630 extraction protocol was replaced by a different one involving sodium carbonate, Flag-tagged AIF1 was again released in conditions of basic pH (pH=10.5), whereas Flag-tagged AIF2 remained attached to the membrane fraction (Fig. 7b). Importantly, in these conditions, endogenous AIF1 (the sole isoform of AIF expressed in HeLa cells) behaved like Flag-tagged AIF1, indicating that membrane-anchoring properties of the recombinant AIF was not affected by the Flag tag (Fig. 7b). Next, we assessed the effect of the alkylating agent MNNG on the release of AIF1 *versus* AIF2. Again, it appeared that Flag-tagged AIF1 was readily released into the cytosol of MNNG-treated cells, while Flag-tagged AIF2 remained attached to mitochondria (Fig. 7c). In these conditions, endogenous AIF1 co-translocated to the cytosol in the presence of Flag-tagged AIF1. However, endogenous AIF1 was withheld from the cytosol in the presence of Flag-tagged AIF2 (Fig. 7c).

We conclude that AIF2 is more difficult to be released from mitochondria than AIF1. This difference cannot be explained by the consensus sequence of the cleavage site by calpains and cathepsins, which is the same for both proteins. Rather, the differential release of AIF1 and AIF2 must be linked to other properties of the molecules such as the accessibility of AIF2 to proteases. Thus, the N-terminus of AIF2 might be more profoundly "buried" in the lipid bilayer of the inner mitochondrial membrane than that of AIF1. In support of this possibility, biochemical studies of AIF1 carried out by Churbanova et al.[27] suggest that redox-regulated changes in the

conformation of AIF that implicate its N-terminal and C-terminal segments might dictate AIF's accessibility to apoptotic proteases and regulate its mitochondrial release in dying cells. In this context, the dimerization of AIF molecules has also been suggested.[27,28] Indeed, endogenous AIF1 could be detected in the anti-Flag immunoprecipitate of Flag-tagged AIF1 or AIF2 (Fig. 7d). Thus, the two AIF isoforms can form homo- or heterodimers or higher-order oligomers. Accordingly, we hypothesize that the inhibitory effect of AIF2 on AIF1 release might be explained by a physical interaction between the two isoforms that makes the mitochondrial release-associated cleavage of AIF1 more difficult to be achieved when AIF2 is present.

Concluding remarks

In this paper, we comparatively analyze two AIF isoforms that solely differ in the utilization of one exon (exon 2) that codes for a portion of the AIF N-terminus. Both AIF isoforms, AIF1 and AIF2, are associated with the inner mitochondrial membrane and are similar in their capacity to sustain a normal function of the respiratory chain. Importantly, it appears that the IMSS of AIF1 (IMSS-AIF1), which is encoded by exon 2a, is cleaved during the import of the AIF precursor into mitochondria, in a highly conserved peptide motif, after residue 54 (in humans AIF1) or residue 53 (in mouse AIF).[6,29] This implies that only 29 amino acids of the C-terminal half of IMSS-AIF1 are present in the mature mitochondrial AIF1 protein. Importantly, mature mitochondrial AIF2 (as present in brain tissues or obtained by transfection with a cDNA) exhibited exactly the same electrophoretic mobility as AIF1, suggesting that AIF2 is trimmed during mitochondrial import by a peptidase that cleaves within the exon 2b-encoded IMSS-AIF2 as well. As a result, the N-terminus of AIF1 and AIF2 are dissimilar in their primary sequence as well as in their hydrophobicity, explaining the relatively loose association of AIF1 (which bears

a less hydrophobic N-terminus than AIF2) with the inner mitochondrial membrane. Consequently, AIF2 is more difficult to dissociate from mitochondrial membranes, irrespective of the nature of the desorbing agent (non-ionic detergents, basic pH or MNNG stimuli), suggesting that AIF2 contributes less efficiently to apoptosis than AIF1.

AIF2 was solely expressed in the developing and adult central nervous system (CNS), as well as in the retina (which contains neurons and, in developmental and anatomical terms, is a CNS derivative). Similarly *AIF2* was present in neuroblastomas but not in any other kind of tumor derived from non-neuronal tissues. While all CNS cells that express *AIF1* also contain *AIF2*, some cells whose exact nature remains to be identified are positive for *AIF2* but not for *AIF1*. What might be the "purpose" of CNS-restricted expression of AIF2 in teleological terms? AIF1 and AIF2 share their vital functions with regard to mitochondrial respiration, while AIF2 is more tightly bound to mitochondrial membranes and hence less likely to mediate cell death (which requires the mitochondrial release and nuclear translocation of AIF). If this hypothesis was correct, the utilization of exon 2b (which gives rise to AIF2) might constitute a strategy to avoid AIF-dependent neurotoxicity. Since AIF1 and 2 can interact with each other and since AIF2 can withhold AIF1 in mitochondria, the putative neuroprotective function of AIF2 would extend to those cells that express both AIF1 and AIF2. For testing this hypothesis, exon 2b-specific knockouts should be generated and evaluated for their putative neurotoxicity alone or upon neuronal injury. As a caveat, it must be mentioned that the expression level of AIF has a profound impact on neuronal differentiation.[12] Therefore, it remains formally possible that AIF2 (but not AIF1) is intimately linked to CNS development and that the exon 2b-specific knockout will cause major brain defects. These intriguing hypotheses will be studied in the future.

Acknowledgments: *EH is supported by a fellowship from the Ligue Nationale contre le Cancer. GK is supported by Grants from European Union (projects Apo-Sys, ChemoRes, Death-Train), La Ligue Nationale Contre le Cancer (équipe labélisée), Institut National du Cancer (INCa), Agence Nationale de Recherche (ANR). FC is supported by Grants from the Telethon Foundation, AIRC and the Italian Ministry of University and Research. PB and PR are supported by Grants from European Union (project EumitoCombat), Leducq foundation. GH is* supported by the German National Genome Research Network (01GS08136-4). *Authors acknowledge the DTP at NCI for providing RNA samples for NCI60 panel of cancer cell lines;* Marcel Leist, University of Konstanz, Germany for providing the LUHMES cells; *Abdelali Jalil, Didier Métivier and Fulvio Florenzano for help with flow cytometry and confocal microscopy; Eric Jacquet and Imagif (CNRS) Platform for quantitative RT/PCR analyses.*

Materials and Methods

Antibodies : The following antibodies were used: anti-actin mouse mAb (CHEMICON, MAB1501); anti-AIF mouse mAb (Santa Cruz, Sc13116); anti-CI SU20 (NDUFB8) mouse mAb (Mitosciences, MS105); CypD mAb (Mitosciences, MSA04); anti-cytochrome C mouse mAb (Pharmingen, 556433); anti-Hsp60 mouse mAb (Stressgen, SPA-806); antiEndoG rabbit pAb (Cell Signaling, 4969); anti-Flag M2 mouse mAb (SIGMA, F3165); anti-Tim23 mAb (BD Transduction, 611222); polyclonal anti-VDAC rabbit pAb (Cell Signaling, 4866); HRP-conjugated goat anti-mouse (Southern Biotech, 1031-05) and goat anti-rabbit (Southern biotech, 4010-05); Alexa fluor 488-conjugated goat anti-mouse (Molecular probe, A11029).

Plasmids and siRNA: Recombinant plasmids pCMV-AIF1-3xFlag and pCMV-AIF2-3xFlag were constructed by cloning AIF1 and AIF2 open reading frames between EcoR1 and kpn1 sites of the vector pCMV-3xFLAG-CMV-14 (Sigma). The plasmid dsRedmito (Clontech) overexpressing a mitochondrion-targeted dsRed fluorescent protein was used for the tagging of mitochondria in transfected cells. The reference plasmid (Ref-AIF1/AIF2) used for the relative quantitation of AIF1 and AIF2 expression level by standard curve method was constructed by simultaneous head-to-tail ligation of AIF1 (1 to 438 bp) and AIF2 (1 to 426 bp) open reading frames and their cloning into Not1 and EcoR1 sites of pGEMTeasy vector (Promega). For RNA interference experiments the following siRNA sequences were used: Negative control (C^-) (AUGCAGAACUCCAAGCACGdTdT), AIF-exon 2a (GGGCAAAAUCGAUAAUUCUdTdT), and AIF 3'UTR (GCAGACUUUCUCUGUGUAUdTdT).

Cell culture and transfection: Human Osteosarcoma U2OS cells (ATCC n°HTB-96) as well as cervix carcinoma Hela cells (ATCC n°CCL-2) were cultured at 37°C and 5% CO_2 in Dulbecco's modified Eagle's medium (Gibco) supplemented with 10% heat-inactivated fetal bovine serum (FBS) (PAA) and 1% penicillin/streptomycin. Mouse embryonic fibroblasts (MEF) were cultured in Dulbecco's modified Eagle's medium (Gibco) supplemented with 10% heat-inactivated FBS (PAA), 1% penicillin/streptomycin (Invitrogen) and 0.01% β-mercaptoethanol. Mouse neural precursor cells (ETNA) were cultured and differentiated *in vitro* according to Cozzolino *et al*.[30] LUHMES (Lund Human Mesencephalic neurons) that were derived by conditional immortalization of female human embryonic ventral mesencephalic cells and subsequent clonal selection, could be differentiated in the presence of GDNF into postmitotic neurons with a robust dopaminergic phenotype.[31] Briefly, LUHMES were cultured in poly-L-lysine (Sigma) and fibronectin (Sigma) (50μg/ml)-coated culture flasks in proliferation medium, namely DMEM/F12 (Sigma) supplemented with 2 mM L-glutamine (Invitrogen), 1% N2 supplement, 25μg/ml bFGF (R&D Systems) and 1% penicillin/streptomycin (Invitrogen). Cells were cultured at a density of 2 x 10^6 and split every 4 or 5 days with proliferation medium changes every 3 days or at 80% confluence. For differentiation, cells were seeded in 6 well plates at a density of 40.000 cells/cm^2 in differentiation medium, namely DMEM/F12, 1% N2 supplement, 1 mg/ml tetracyclin (Sigma), 49 mg/ml dibutyryl-cAMP (R&D Systems), and 5 ng/μl GDNF (R&D Systems). Every day and up to 6 days after the onset of differentiation, 6 wells were pooled for RNA extraction.

Plasmid and siRNA transfections were performed using Lipofectamine-2000 reagent (Invitrogen) by following manufacturer's procedure. Pools of stably transfected U2OS cells expressing AIF1-Flag or AIF2-Flag were established by co-transfection with the plasmids

described above and the pPuro plasmid (Clontech) followed by selection in the presence of 0.25 μg/ml of puromycin (Clontech) and 0.5 mg/ml of Geneticin (Invitrogen).

Cell lysates preparation, immunoprecipitation and Western blot analyses: For whole extract preparation, cells were harvested, washed three times with ice-cold PBS (8.1 mM Na_2HPO_4, 135 mM NaCl, 1.5 mM KH_2PO_4, 2.7 mM KCl), lysed with 1% SDS, boiled, sonicated, and stored at -80°C. Proteins contained in the lysate were quantified (DC protein assay; Biorad) and resolved directly by SDS/PAGE (NUPAGE; Invitrogen) and then subjected to Western blot analyses following manufacturer reagents and instructions (Invitrogen). For immunoprecipitations, cells were lysed for 20 minutes at 4°C in the following buffer: NetN-120 (20 mM Tris-HCl at pH 8.0, 120 mM NaCl, 1 mM EDTA, 0.5 % Igepal CA 630) supplemented with protease (EDTA-free protease inhibitor tablets - Roche) and phosphatase (Phosphatase inhibitor tablets - Roche) inhibitors. After centrifugation (13,000xg for 10 min at 4°C), the protein content in the lysates was quantified and used for immunoprecipitations. The following immunoprecipitation procedure was used: first protein G-Sepharose CL-4B beads (50 μl of a 50 % slurry, GE Healthcare) were coated with 1 μg of the indicated antibody, by incubating for 2 h at 4°C in 800 μl of binding buffer (20 mM Tris-HCl pH 8.0, 120 mM NaCl, 1 mM EDTA, 0.5 % Igepal). Then, antibody-coated beads were washed three times in binding buffer and incubated for 2 h at 4°C with 300 μg of cell lysate, in a final volume of 800 μl. Beads were finally washed four times with lysis buffer and co-immunoprecipitated proteins were released by boiling in SB (2 % SDS, 10 % glycerol, 62.5 mM Tris-HCl pH 6.8, 100 mM dithiothreitol), resolved by SDS/PAGE and then subjected to Western blot analysis. For Western blot analysis, SDS/PAGE-resolved proteins were transferred onto nitrocellulose membrane (Biorad). Membranes were blocked by incubating

with 5% nonfat milk powder in TBST buffer (10 mM Tris-HCl pH 8.0, 150 mM NaCl, 0.05 % Tween 20) for 1h, and then for further 16 h at 4°C with the specified primary antibody diluted in the same incubation mixture supplemented with 0.02% Na-azide. The membrane was then washed three times in TBST buffer before incubation with a horseradish peroxidase-conjugated secondary antibody. Antibody binding was detected with the ECL+ chemiluminescence detection kit (GE Healthcare).

Indirect immunofluorescence analyses: Cells were fixed on coverslips for 30 min with 4% PFA /2% Sucrose/0.19% Picric acid, then permeabilized for 5 min with Triton 0.2% at room temperature. Flag-tagged proteins were detected by incubation with an anti-Flag mAb (1:8000 dilution), followed by Alexa fluor 488-conjugated goat anti-mouse. We stained the DNA in the samples with 1 μM TOPRO3 (Invitrogen). Samples slides were then mounted using the reagent Fluoromont-G (Southern Biotech) and observed by confocal microscopy with a Leica TSC-SPE confocal microscope equipped with a 63x/1.15 Olympus objective and a Leica Aplication Suite (LAS) software (Leica Microsystems). For the submitochondrial localization of AIF2, pools of stably transfected U2OS cells overexpressing AIF1-Flag ou AIF2-Flag were first fixed for 30 min with 4% PFA /2% Sucrose/0.19% Picric acid then permeabilized for 5 min without or with 0.4 and 0.8 mg/ml of digitonin. Flag-tagged proteins were detected by incubation with an anti-Flag mAb (1:8000 dilution), followed by a Alexa fluor 488-conjugated goat anti-mouse. Anti-Tim23 mab and CypD mab were used for the detection of respectively mitochondrial inner membrane and matrix. DNA in the samples was stained with TOPRO3. Samples were then mounted and observed with a Leica TSC-SPE confocal microscope.

RNA Isolation and gene expression analysis by quantitative real-time PCR (qRT-PCR): Total RNA purified from normal human organs or brain sub-regions were purchased from Clonetech. Total RNA from wild type (wt) or harlequin (Hq) mutant mice organs were extracted using Precellys homogenizer (Bertin) and RNA isolation kit from Qiagen. RNA from human and mouse cells in culture were extracted using PARIS kit (Ambion) or "Total RNA Isolation Kit II" (Macherey Nagel). All RNA samples were then stored at -80°C. The quantification of RNA samples was achieved using the Nanodrop ND-1000 Spectrophotometer and the integrity of the RNA was verified using the Agilent 2100 Bioanalyzer with the Eukaryote Total RNA Nano assay. One microgram of total RNA was reverse-transcribed in a 20μl final reaction volume using the High Capacity cDNA Reverse Transcription Kit with RNase inhibitor (Applied Biosystems) following the manufacturer's instructions. For the human and mouse AIF1 and AIF2, the following primers and Taqman MGB probes were custom-made by Applied Biosystems: human AIF1 primer (AIF1F): 5'GGCAAAATCGATAATTCTGTGTTAGTC3'; human AIF2 primer (AIF2F): 5'GGAAAGATGGCAGCAACCTAGTGTACT3'; human AIF commun primer (AIFcr): 5'CCACCAATTAGCAGGAAAGGAA 3'; human AIF commun probe (AIFcp): 5' TGTTTCTGTTCTGGTGTCAG 3'; mouse AIF1 primer (AIF1R): 5'CCATTGCTGGAACAAGTTGC 3'; mouse AIF2 primer (AIF2R): 5'CTAGGAGATGACACTGCACAA 3'; mouse AIF commun primer (AIFcF): 5'CGAGCCCGTGGTATTCGA 3'; mouse AIF commun probe (AIFSc): 5' ACGGTGCGTGGAAG 3'. TaqMan® probes were labeled with 6-FAM at the 5' end and with a nonfluorescent MGB quencher at the 3' end. Each probe was combined with different forward and reverse primers (see list) for AIF1 or AIF2 quantification. TaqMan® gene expression assays for 18S ribosomal RNA (Hs99999901_s1), GAPDH (Mm99999915_g1), PGK1

(Mm00435617_m1), TBP (Mm00446973_m1) and the TaqMan® Mouse Endogenous Control Arrays (384-well micro fluidic card containing 16 mouse TaqMan® Gene Expression Assays) were from Applied Biosystems. Quantitative PCR reactions were performed using ABI Prism 7900 HT sequence detection system (Applied Biosystems). For microplate experiments, 25 ng of cDNA were used as template for q-PCR reactions with TaqMan® Universal Master Mix (Applied Biosystems), 900 nM primers and 200 nM probes. Real-time q-PCR amplifications were carried out (10 min 95°C followed by 45 cycles of 15 sec 95°C and 1 min 60°C). Technical replicates were performed for each biological sample. For the micro fluidic Taqman® arrays, 100 ng of cDNA were used per sample-loading ports, each allowing 48 q-PCR reactions using manufacturer instructions (10 min 94.5°C followed by 40 cycles of 30 sec 97°C and 1 min 59.7°C). For AIF1 and AIF2 expression quantification in differentiating mouse neural cells, reference genes were selected using the TaqMan® Mouse Endogenous Control Arrays. Briefly, 16 housekeeping genes were tested in triplicate for each sample. The most stable genes were selected by analyzing results with GeNorm and Normfinder functions in Genex 4.3.8 (MultiD, Göteborg, Sweden). The geometric mean of the 3 best housekeeping genes (*GAPDH*, *PGK1* and *TBP*) was used to normalize gene expression levels of AIF1 and AIF2 for further analysis of microplate q-PCR experiments with the relative quantification method. For AIF1 and AIF2 expression quantification in human samples, absolute quantification experiment were performed using standard curves obtained by a ten-fold dilution series of a pBlueREF-AIF1+2 plasmid. Obtained Ct values for each human sample allowed AIF1 and AIF2 quantifications according to the standard curves using SDS 2.3 software (Applied Biosystems). Determined quantity values were then exploited for further analysis.

Mice manipulation: Wild type male CD-1 mice of 3-5 months age were used for the *in situ* hybridization experiments. Animals were anesthetized with Avertin (0.25 mg/g body weight, intraperitoneally) and perfused through the heart sequentially, first with PBS (pH 7.4) and then with 4% paraformaldehyde (PFA). The brains were post-fixed for 24 h at 4°C and cryoprotected with 30% sucrose/PBS for 48 h at 4°C. Coronal and sagittal cryosections (18-20 μm thick) were obtained by using a cryostat and collected at -80°C.

In situ *hybridization*: The cDNA fragments of mouse AIF1 and AIF2 isoforms (NM_012019 and CX_238424) were obtained by RT/PCR from total RNA extracted from adult mouse brain, using the following primers: AIF1 forward 5'-GCAACTTGTTCCAGCAATGGC-3' and reverse 5'-gcaccagctcctattgttgataagc-3'; AIF2 forward 5'-GCAGTGTCATCTCCTAGGATC-3' and reverse 5'-ATAAATTCCTGCCCCAGTCAC-3'. Different cDNAs were subcloned into the pGemT-easy vector (Promega). The digoxigenin (DIG)- and biotin (BIO)-labeled riboprobes were produced using these plasmids as templates for the *in vitro* transcription according to the manufacturer's instructions (Roche). Cryosections were fixed in 4% PFA for 15 min, then treated with proteinase K (20 μg/ml) and with 0,2% glycine for 5 min, respectively. A second fixing with 4% PFA and 0,2% glutaraldehyde was followed. The sections were pre-hybridized at 55°C for 2 h in the hybridization buffer (50% formamide, 5x SSC, 10% blocking reagent, 5mM EDTA, 0.1% Tween-20, 0.1% CHAPS, 0.1mg/ml heparin, 1mg/ml yeast RNA). The probes labeled with digoxigenin (DIG) or biotin (BIO) were added to the hybridization mix at concentrations of 1ng/μl and 15 ng/μl in the colorimetric and fluorescence *in situ* hybridization, respectively. The sections were incubated with this solution at 55°C over night. The sections were sequentially washed in 2x SSC/50% formamide at 50°C, three times for 30 min, and then in

PBS at room temperature. In the colorimetric *in situ* hybridization, alkaline phosphatase-conjugated anti-DIG antibody and the chromogenic substrate NBT/BCIP were used to detect the DIG-labeled probe, according to the manufacter's protocol (Roche). Images were captured using a Nikon SMZ 800 microscope equipped with Nikon Coolpix 995 digital camera. In the fluorescence *in situ* hybridization, the sections were incubated with the anti-DIG antibody conjugated with Cy3 at concentration of 1:100 (Jackson Immunoresearch) for 2 h at room temperature for the detection of the DIG-labeled probe. After three washes in PBS, the sections were incubated for 30 min at room temperature with the streptavidin conjugated with Alexa488 at concentration of 1:100 (Invitrogen) to detect the BIO-labeled probe. There were no apparent signals in control sections with the sense probes. The fluorescence was acquired by using a confocal laser scanning microscope (Leica). The brightness and contrast were adjusted using LAS software (Leica Microsystems).

Differential Mitochondrial membrane permeabilization using with non ionic detergent: Mouse embryonic fibroblasts (MEF) transiently overexpressing AIF1-Flag or AIF2-Flag were incubated for 30 min in buffer A (20 mM Tris pH8, 120 mM NaCl, 1 mM EDTA) or buffer A supplemented with 0.03% - 0.06% - 0.1% of Igepal CA-630 (Sigma). Membrane-bound proteins were separated from soluble proteins by 10 min centrifugation at 13 000 g and analyzed by Western blot.

Mitochondria purification: Cells were incubated for 20 min in a hypotonic buffer (10 mM Hepes-KOH, pH 7.9 ; 1.5 mM $MgCl_2$; 10 mM KCl ; 0.5 mM DTT) supplemented with protease and phosphatase inhibitors (1 tablet/10ml, Roche). Cells were then lysed with a Dounce

homogenizer and centrifuged for 10 min at 700 g. The corresponding supernatant was transferred to a fresh tube and centrifuged for an additional 15 min at 12 000 g. The pellet, which corresponded to the mitochondrial fraction, was washed 1x with the hypotonic buffer and lysed with 1% SDS.

Mitochondrial membrane solubilization at high pH (Na_2CO3 treatment): Mitochondria were purified from Hela cells transiently overexpressing AIF1-Flag or AIF2-Flag as described above. The post-centrifugation mitochondria-enriched pellet was resuspended and incubated for 20 min in 100 mM Na_2CO_3 (pH 10,5) and then centrifuged for 1h at 65000 rpm. Solubilized proteins contained in the supernatant (S) and those still bound to membranes contained in the pellet (P) were lysed 1% SDS (diluted in 100 mM Na_2CO3, pH 10.5) and analyzed by Western blotting.

Membrane/Cytosol fraction separation: Hela cells overexpressing AIF1-Flag or AIF2-Flag were incubated for 20 min in a hypotonic buffer (10 mM Hepes-KOH pH 7.9; 1.5 mM $MgCl_2$; 10 mM KCl and 0.5 mM DTT) supplemented with protease and phosphatase inhibitors. Cells were then lysed with a Dounce homogenizer and centrifuged for 15 min at 12 000 g. The pellet, corresponding to the membrane fraction, was washed 1x with the hypotonic buffer before being lyzed in the same buffer supplemented with 1% SDS. The supernatant was re-centrifuged at 65000 rpm for 1h supplemented with 1% SDS and used as the cytosolic fraction. To study the mitochondrial release of AIF1 and AIF2 after treatment with MNNG (*N*-Methyl-*N*'-Nitro-*N*-Nitrosoguanidine), Hela cells were treated for 15 min with 500 μM before being re-incubated at 37°C with the complet drug-medium for 4 hr and processed for membrane/ cytosol fractionation.

Assessment of respiratory chain function: A first spectrophotometric assay was used to successively measure the activity of complex IV (cyanide-sensitive cytochrome c oxidase), complex II+III (malonate-sensitive succinate cytochrome c reductase) and complex III (antimycin-sensitive decylubiquinol cytochrome c reductase) in 400 µl of medium containing 10 mM KH_2PO_4, pH 7.2) and 1 mg/ml BSA.[32] This assay measures the redox changes of cytochrome c using two wavelengths (550 nm–540 nm). A second assay successively measuring the activity of complex I (rotenone-sensitive decylubiquinone NADH reductase) and V (oligomycin-sensitive ATPase) was performed in 320 µl of water to which is added 80 µl of medium consisting of 50 mM Tris (pH 8.0), and 5 mg/ml BSA. It measures NADH oxidation at wavelengths of 340 nm–380 nm as previously described.[32] All measurements were carried out using a Cary 50 spectrophotometer equipped with an 18-cell holder maintained at 37 °C. All chemicals were of the highest grade from Sigma Chemical Company (St Louis).

Electron Microscopy: Cells were fixed in phosphate buffer pH 7.2 - 3% glutaraldehyde for 1 h, and postfixed in 0.1M cacodylate buffer – 1% osmium tetroxyde for 2 h. After being rinsed for 5 min in water and 15 min in the 0.1M cacodylate buffer, cells were transferred to 0.2 M cacodylate buffer for 30 min. Cells were washed in 30% methanol for 10 min, stained in 2% uranyl acetate in 0.1M cacodylate buffer – 30% methanol for 1 h, and washed in 30% methanol. Cells were then dehydrated in increasing concentrations of ethanol and embedded in Epon 812. For observations, ultrathin sections were contrasted with 4% uranyl acetate and lead citrate and examined with a FEI Technaï 12 microscope at 80 Kv.[33]

REFERENCES

1. Susin SA, Lorenzo HK, Zamzami N, Marzo I, Snow BE, Brothers GM *et al*. Molecular characterization of mitochondrial apoptosis-inducing factor. *Nature* 1999; **397**: 441-446.

2. Mate MJ, Ortiz-Lombardia M, Boitel B, Haouz A, Tello D, Susin SA *et al*. The crystal structure of the mouse apoptosis-inducing factor AIF. *Nat Struct Biol* 2002; **9**: 442-446.

3. Ye H, Cande C, Stephanou NC, Jiang S, Gurbuxani S, Larochette N *et al*. DNA binding is required for the apoptogenic action of apoptosis inducing factor. *Nat Struct Biol* 2002; **9**: 680-684.

4. Modjtahedi N, Giordanetto F, Madeo F, Kroemer G. Apoptosis-inducing factor: vital and lethal. *Trends Cell Biol* 2006; **16**: 264-272.

5. Joza N, Pospisilik JA, Hangen E, Hanada T, Modjtahedi N, Penninger J *et al*. AIF: Not just an Apoptosis-Inducing Factor. *Ann. N.Y. Acad. Sci.* 2009; **in press**:

6. Otera H, Ohsakaya S, Nagaura Z, Ishihara N, Mihara K. Export of mitochondrial AIF in response to proapoptotic stimuli depends on processing at the intermembrane space. *EMBO J* 2005; **24**: 1375-1386.

7. Miramar MD, Costantini P, Ravagnan L, Saraiva LM, Haouzi D, Brothers G *et al*. NADH oxidase activity of mitochondrial apoptosis-inducing factor. *J Biol Chem* 2001; **276**: 16391-16398.

8. Vahsen N, Cande C, Briere JJ, Benit P, Joza N, Larochette N *et al*. AIF deficiency compromises oxidative phosphorylation. *EMBO J* 2004; **23**: 4679-4689.

9. Klein JA, Longo-Guess CM, Rossmann MP, Seburn KL, Hurd RE, Frankel WN *et al*. The harlequin mouse mutation downregulates apoptosis-inducing factor. *Nature* 2002; **419**: 367-374.

10. Joza N, Oudit GY, Brown D, Benit P, Kassiri Z, Vahsen N *et al*. Muscle-specific loss of apoptosis-inducing factor leads to mitochondrial dysfunction, skeletal muscle atrophy, and dilated cardiomyopathy. *Mol Cell Biol* 2005; **25**: 10261-10272.

11. Cheung EC, Joza N, Steenaart NA, McClellan KA, Neuspiel M, McNamara S *et al*. Dissociating the dual roles of apoptosis-inducing factor in maintaining mitochondrial structure and apoptosis. *EMBO J* 2006; **25**: 4061-4073.

12. Ishimura R, Martin GR, Ackerman SL. Loss of apoptosis-inducing factor results in cell-type-specific neurogenesis defects. *J Neurosci* 2008; **28**: 4938-4948.

13. van Empel VP, Bertrand AT, van der Nagel R, Kostin S, Doevendans PA, Crijns HJ *et al*. Downregulation of apoptosis-inducing factor in harlequin mutant mice sensitizes the myocardium to oxidative stress-related cell death and pressure overload-induced decompensation. *Circ Res* 2005; **96**: e92-e101.

14. Benit P, Goncalves S, Dassa EP, Briere JJ, Rustin P. The variability of the harlequin mouse phenotype resembles that of human mitochondrial-complex I-deficiency syndromes. *PLoS ONE* 2008; **3**: e3208.

15. Vahsen N, Cande C, Dupaigne P, Giordanetto F, Kroemer RT, Herker E *et al*. Physical interaction of apoptosis-inducing factor with DNA and RNA. *Oncogene* 2006; **25**: 1763-1774.

16. Cande C, Vahsen N, Kouranti I, Schmitt E, Daugas E, Spahr C *et al*. AIF and cyclophilin A cooperate in apoptosis-associated chromatinolysis. *Oncogene* 2004; **23**: 1514-1521.

17. Gogvadze V, Orrenius S, Zhivotovsky B. Multiple pathways of cytochrome c release from mitochondria in apoptosis. *Biochim Biophys Acta* 2006; **1757**: 639-647.

18. Norberg E, Gogvadze V, Ott M, Horn M, Uhlen P, Orrenius S *et al*. An increase in intracellular Ca2+ is required for the activation of mitochondrial calpain to release AIF during cell death. *Cell Death Differ* 2008; **15**: 1857-1864.

19. Gurbuxani S, Schmitt E, Cande C, Parcellier A, Hammann A, Daugas E *et al*. Heat shock protein 70 binding inhibits the nuclear import of apoptosis-inducing factor. *Oncogene* 2003; **22**: 6669-6678.

20. Zhu C, Wang X, Deinum J, Huang Z, Gao J, Modjtahedi N *et al*. Cyclophilin A participates in the nuclear translocation of apoptosis-inducing factor in neurons after cerebral hypoxia-ischemia. *J Exp Med* 2007; **204**: 1741-1748.

21. Galluzzi L, Blomgren K, Kroemer G. Mitochondrial membrane permeabilization in neuronal injury. *Nat Rev Neurosci* 2009; **10**: 481-494.

22. Schulthess FT, Katz S, Ardestani A, Kawahira H, Georgia S, Bosco D *et al*. Deletion of the mitochondrial flavoprotein apoptosis inducing factor (AIF) induces beta-cell apoptosis and impairs beta-cell mass. *PLoS ONE* 2009; **4**: e4394.

23. Loeffler M, Daugas E, Susin SA, Zamzami N, Metivier D, Nieminen AL *et al*. Dominant cell death induction by extramitochondrially targeted apoptosis-inducing factor. *FASEB J* 2001; **15**: 758-767.

24. Delettre C, Yuste VJ, Moubarak RS, Bras M, Lesbordes-Brion JC, Petres S *et al*. AIFsh, a novel apoptosis-inducing factor (AIF) pro-apoptotic isoform with potential pathological relevance in human cancer. *J Biol Chem* 2006; **281**: 6413-6427.

25. Delettre C, Yuste VJ, Moubarak RS, Bras M, Robert N, Susin SA. Identification and characterization of AIFsh2, a mitochondrial apoptosis-inducing factor (AIF) isoform with NADH oxidase activity. *J Biol Chem* 2006; **281**: 18507-18518.

26. Urbano A, Lakshmanan U, Choo PH, Kwan JC, Ng PY, Guo K *et al*. AIF suppresses chemical stress-induced apoptosis and maintains the transformed state of tumor cells. *EMBO J* 2005; **24**: 2815-2826.

27. Churbanova IY, Sevrioukova IF. Redox-dependent changes in molecular properties of mitochondrial apoptosis-inducing factor. *J Biol Chem* 2008; **283**: 5622-5631.

28. Sevrioukova IF. Redox-Linked Conformational Dynamics in Apoptosis-Inducing Factor. *J Mol Biol* 2009;

29. Yuste VJ, Moubarak RS, Delettre C, Bras M, Sancho P, Robert N *et al*. Cysteine protease inhibition prevents mitochondrial apoptosis-inducing factor (AIF) release. *Cell Death Differ* 2005; **12**: 1445-1448.

30. Cozzolino M, Ferraro E, Ferri A, Rigamonti D, Quondamatteo F, Ding H *et al*. Apoptosome inactivation rescues proneural and neural cells from neurodegeneration. *Cell Death Differ* 2004; **11**: 1179-1191.

31. Lotharius J, Falsig J, van Beek J, Payne S, Dringen R, Brundin P *et al*. Progressive degeneration of human mesencephalic neuron-derived cells triggered by dopamine-dependent oxidative stress is dependent on the mixed-lineage kinase pathway. *J Neurosci* 2005; **25**: 6329-6342.

32. Benit P, Goncalves S, Philippe Dassa E, Briere JJ, Martin G, Rustin P. Three spectrophotometric assays for the measurement of the five respiratory chain complexes in minuscule biological samples. *Clin Chim Acta* 2006; **374**: 81-86.

33. Luft JH. Improvements in epoxy resin embedding methods. *J Biophys Biochem Cytol* 1961; **9**: 409-414.

TITLES AND LEGENDS TO FIGURES

Figure 1: Comparison of AIF1 and AIF2 sequences. (a) AIF1 and AIF2 are alternative splice variants transcribed from AIF locus. Alternative usage of exon-2a or -2b of *AIF* gene allows the synthesis of respectively AIF1 and AIF2 isoforms. Human AIF1 and AIF2 share an identical N-terminal (aa 1-35) mitochondrial localization signal (MLS) but bear different inner membrane sorting signal (IMSS-AIF1: aa 35-82 and IMSS-AIF2: aa 35-78) encoded respectively by exon-2a and -2b. The rest of the protein is identical for both isoforms. Primary amino acid sequence comparison for MLS and IMSS regions of AIF1 and AIF2 was achieved using DNASTAR multiple alignment program. Residues differing between the two isoforms are colored in red. (**b) Phylogenetic analyses of AIF1 and AIF2.** Mutiple alignment of exon 2-encoded polypeptides, available from public databases, reveals a restricted simultaneous usage of exon-2a and -2b to mammals. Chicken AIF protein is rooted to mammalian AIF2. This tree is obtained using neighbor joining method after clustalW multiple alignment. Refseq identifiers for analyzed protein sequences are the followings: *Homo sapiens* AIF1 (NP_004199), AIF2 (NP_665811); *Macaca mulata* AIF1 (XP_001092146), AIF2 (XP_001092025); *Equus Caballus* AIF1 (XP_001915191), AIF2 (XP_001915198); *Canis familiaris* AIF1 (XP_538170), (AIF2 XP_865808); *Mus musculus* AIF1 (NP_036149), AIF2 (CAM22220); *Rattus norvegicus* AIF1 (NP_112646), AIF2 (EDM10916); *Gallus gallus* AIF (NP_001007491). (**c) AIF1-IMSS and AIF2-IMSS share conserved amino acids**. Multiple alignment of exon-2a-encoded against exon-2b-encoded polypeptide segments, from the same organisms presented in 1b, was achieved using clustalW multiple alignment program. Star indicates fully conserved residues. Dots indicate residues with similar properties. The histogram of residue conservation is presented at

the bottom of the figure. (**d) Prediction of secondary structural characteristics and physicochemical properties of the N-terminal segments of AIF1 and AIF2.** Entire primary amino acid sequences of AIF1 and AIF2 were analyzed using DNASTAR Protean Secondary structure prediction program and only the result for the N-terminal segment (MLS + IMSS) of each isoform is shown.

Figure 2: AIF2 mRNA expression is restricted to the brain. Quantitative expression analyses of AIF1 and AIF2 mRNAs in various human (**a**) and murine (**c**) organs or in various human brain sub-regions (**b**) were performed. AIF1 and AIF2 mRNA expression was compared between brains of wild type (wt) and hypomorphic Harlequin (Hq) mutant mice (**d**). Data obtained for human samples (a and b) correspond to three independent quantifications (mean $\pm$ SD) and for mouse organs (c and d) represent means $\pm$ SD from at least three independent experiments. Relative quantification of AIF1 and AIF2 mRNA expression levels in human samples (**a, b**) was achieved by standard curve method using an AIF1/AIF2 reference plasmid. For murine RNA samples, relative fold variation of AIF1 and AIF2 were calculated using the comparative C_t method.

Figure 3: Expression of AIF2 during neuronal differentiation. Murine neural precursor cells (ETNA) were differentiated *in vitro* into neurons (**a**) (Bar represents 20 μm) and AIF1 and AIF2 mRNA expression levels were compared between undifferentiated, solvent-treated and differentiated cells (**b**). Data represents three independent experiments (mean $\pm$ SD). Human mesencephalic cells (LUHMES) were differentiated *in vitro* into postmitotic dopaminergic neurons and AIF1 and AIF2 mRNA expression levels were compared in RNA samples prepared

every day, from day 0 (undifferentiated) up to day 6 after the onset of differentiation (**g**). Data result from two independent quantifications (means ± SD).

Figure 4: AIF1 and AIF2 mRNA expression profile in cancer cells. Quantitative expression levels of AIF1 and AIF2 mRNAs were measured in human neurablastoma (IMR32, SHSY5Y and SK-N-AS) and glioblastoma (A172 and NCI60 panel: SF-268, SF-295, SF-539, SNB-19, SNB-75 and U251) cell lines (**a**) as well as primary human neuroblastoma tumors (**b**). Means ± SD are obtained from two independent experiments.

Figure 5: AIF1 and AIF2 mRNA expression pattern in mouse brain. (**a-f**) Parallel *in situ* hybridization using respectively AIF1 (**a, c, e**) and AIF2 (**b, d, f**) specific probes on brain sagittal sections (**a** and **b**) or the mitral and granular cell layers of the olfactory bulb (**c** and **d**) and cortex (**e** and **f**) on coronal sections (Bar =1 mm). (**g-i**) dual fluorescent *in situ* hybridization, with AIF1 (red) (**g**) and AIF2 (green) (**h**) probes, on the anterior olfactory nucleus (aon) area of brain in sagittal section. The arrows indicate positive cells only for AIF2 in merged images **(i)** (Bar=20 μm). *aon, anterior olfactory nucleus; gl, glomerular layer; gro, granular cell layer; mi, mitral cell layer; tu, olfactory tubercle; pir, piriform cortex.*

Figure 6: (a) AIF2 is targeted to mitochondria. HeLa cells transiently co-transfected with the mitochondrial marker dsRed-mito (red fluorescence) and pCMV-AIF1-Flag (top panel) or pCMV-AIF2-Flag (bottom panel) were fixed, immunostained using an anti-Flag antibody (green), counterstained with the DNA-specific dye TOPRO3 for the determination of nuclear area and then observed by confocal microscopy; **(b) AIF1 and AIF2 are localized in the same**

sub-mitochondrial compartment. U20S cells stably overexpressing AIF1-Flag or AIF2-Flag were permeabilized with various concentrations of digitonin and mitochondrial proteins were detected using anti-Flag (AIF1-Flag and AIF2-Flag), anti-Tim23 (inner membrane protein Tim23) and anti-CypD (Matrix protein CypD) by confocal microscopy**; (c) Histogram of the frequency of cells positively immunostained with each antibody for all permeabilization conditions used in (c); (d) Both AIF1 and AIF2 regulate mitochondrial respiratory chain complex I subunits.** Western blot analysis of complex I subunit CI SU20 (NDUFB8). Whole lysates of U20S cells cotransfected with control siRNA, or AIF siRNA (AIF exon2a or AIF 3'UTR) in the presence of empty vector (Flag) or recombinant plasmid pCMV-AIF1-Flag (AIF1-Flag) or pCMV-AIF2-Flag (AIF2-Flag) were subjected to Western blot detection of indicated proteins. Bar =5 μm.

Figure 7: Membrane anchorage capacity of AIF1 and AIF2. (a) Detergent-induced permeabilization of mitochondrial membranes. MEF cells transiently transfected with vector (Flag), pCMV-AIF1-Flag (AIF1-Flag) or pCMV-AIF2-Flag (AIF2-Flag) were incubated without or with increasing concentrations of Igepal CA-630 and then ultracentrifuged to separate the soluble fraction (Supernatant) from the membrane fraction (Pellet). Proteins in both fractions were separated by SDS-PAGE and then analyzed by Western blot using antibodies for the indicated proteins. (**b) High pH-dependent mitochondrial membrane solubilization.** Mitochondria were first purified from HeLa cells overexpressing AIF1-Flag or AIF2-Flag and then incubated with 100 mM Na-carbonate (pH 10.5). After centrifugation, supernatant (S) as well as pellet (P) fractions were subjected to SDS/PAGE and Western blot analyses using the indicated antibodies. (**c) Mitochondrial release of AIF1 and AIF2 in MNNG treated cells.**

HeLa cells overexpressing AIF1-Flag or AIF2-Flag were treated with DMSO or with the alkylating agent MNNG and then lysed under hypotonic buffer conditions. Cytosolic and membrane fractions obtained after high-speed ultracentrifugation were then subjected to SDS/PAGE and Western blot analyses using the indicated antibodies. (**d) AIF1 and AIF2 dimerization.** HeLa cells transiently transfected with vector (Flag), pCMV-AIF1-Flag (AIF1-Flag) or pCMV-AIF2-Flag (AIF2-Flag) were lysed and submitted to immunoprecipitation using the indicated antibodies. Whole cell lysates (Input) as well as co-immunoprecipitated proteins were then resolved by SDS-PAGE and submitted to Western blot analyses using the indicated antibodies. Arrows indicate the electrophoretic position of Flag-tagged and endogenous AIF proteins.

Supplemental figure informations

A brain-specific isoform of mitochondrial Apoptosis Inducing Factor: AIF2

Hangen et al.

Supplemental figure 1: AIF1 isoform mRNA expression in NCI60 panel cancer cell lines. Quantitative expression analysis of AIF1 mRNA in NCI60 panel of human cancer cell lines, originated from various tissues, was achieved and relative fold variation of AIF1 in analyzed cell lines was calculated using the comparative C_t method. The 18S RNA was used as the endogenous reference.

Supplemental figure 2: *in situ* hybridization controls. Results using control sense probes for AIF1 (a, c, e) and AIF2 (b, d, f) on brain saggital sections (a and b), the mitral and granular cell layers of the olfactory bulb (c and d) and cortex (e and f) on coronal sections is displayed.

Supplemental figure 3: Failure of AIF depletion to affect NAD(P)H levels in neuroblastoma cells. Cytofluorometric determination of baseline levels of NAD(P)H in SHSY-5Y neuroblastoma cells transfected with a control siRNAs or siRNAs that have been designed to deplete AIF1, AIF2 or both (same siRNAs as Fig. 6d). Then, the autofluorescence of cells (excitation 360 nM, emission 530 nm) was determined as an estimate of the intracellular NAD(P)H concentration. This experiment has been repeated three times, yielding similar results.

Supplemental figure 4: Overexpression of AIF1-Flag and AIF2-Flag differentially affects mitochondrial ultrastructure. Untransfected U20S cells or pools of stably transfected cells with the empty vector (vector) or pCMV-AIF1-Flag (AIF1-Flag) or pCMV-AIF2-Flag (AIF2-Flag) were analyzed for recombinant Flag-tagged AIF expression (a), the activity of mitochondrial respiratory chain complexes (CI to CV) (b) and mitochondrial ultrastructure by transmission electron microscopy (c).

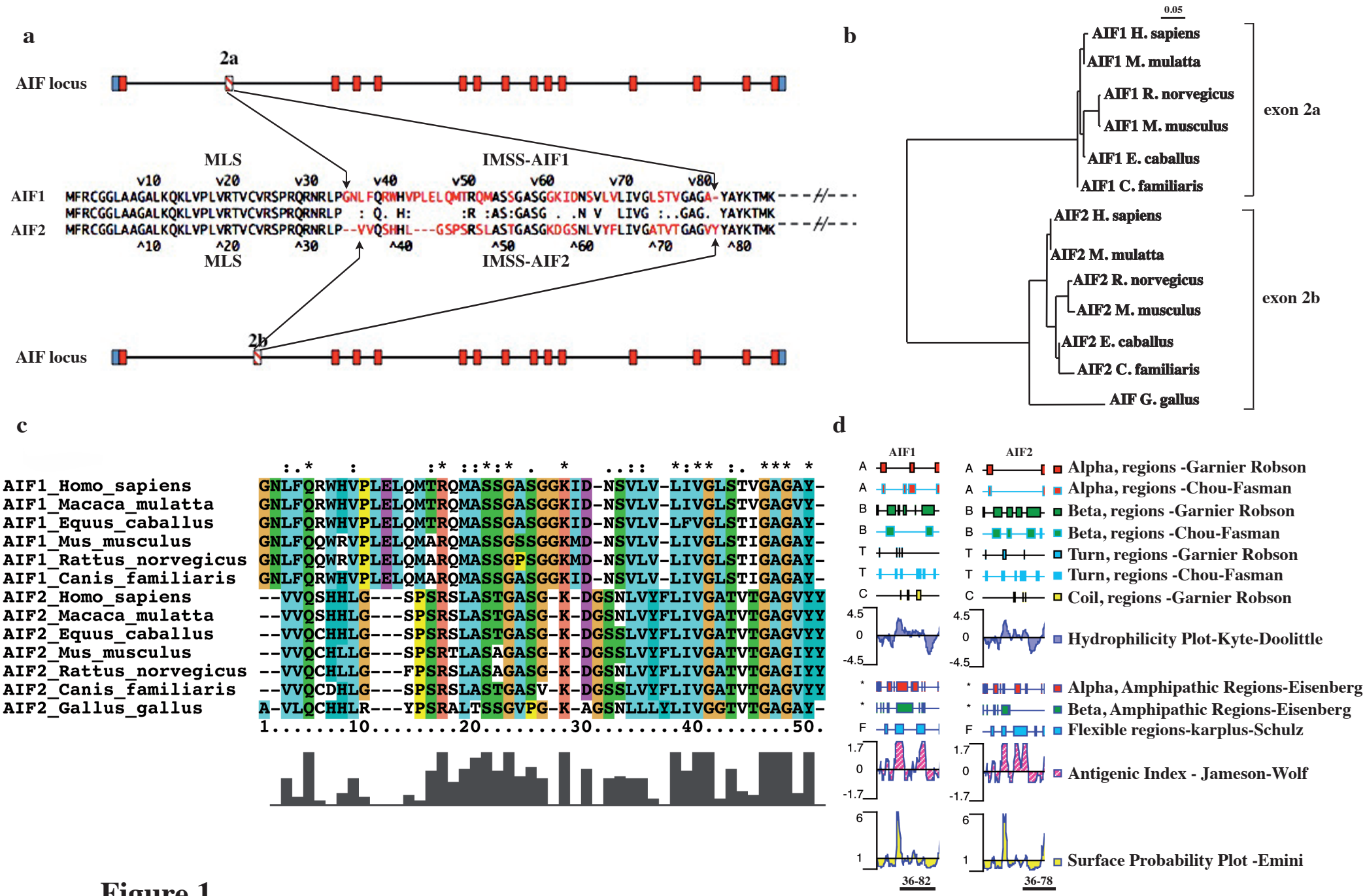

Figure 1

Hangen et al.

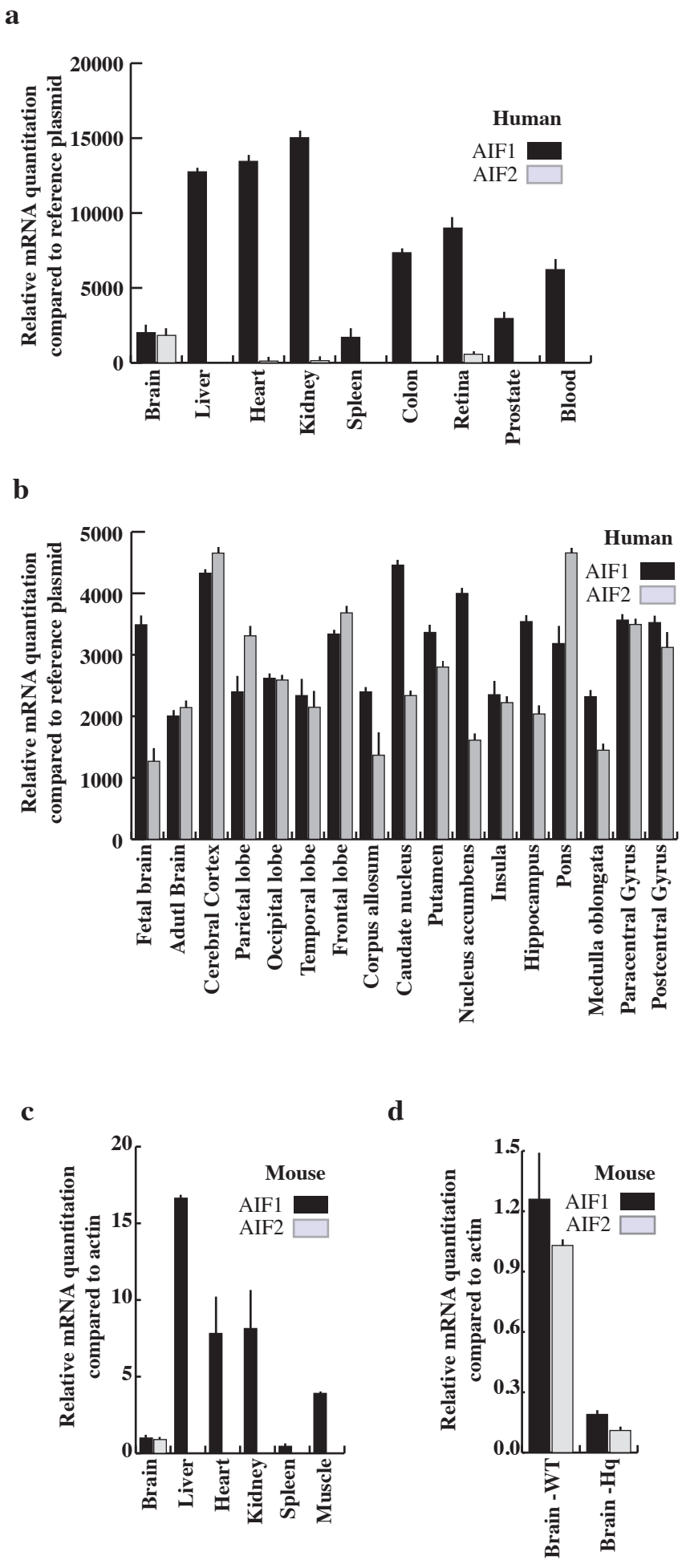

Figure 2
Hangen et al

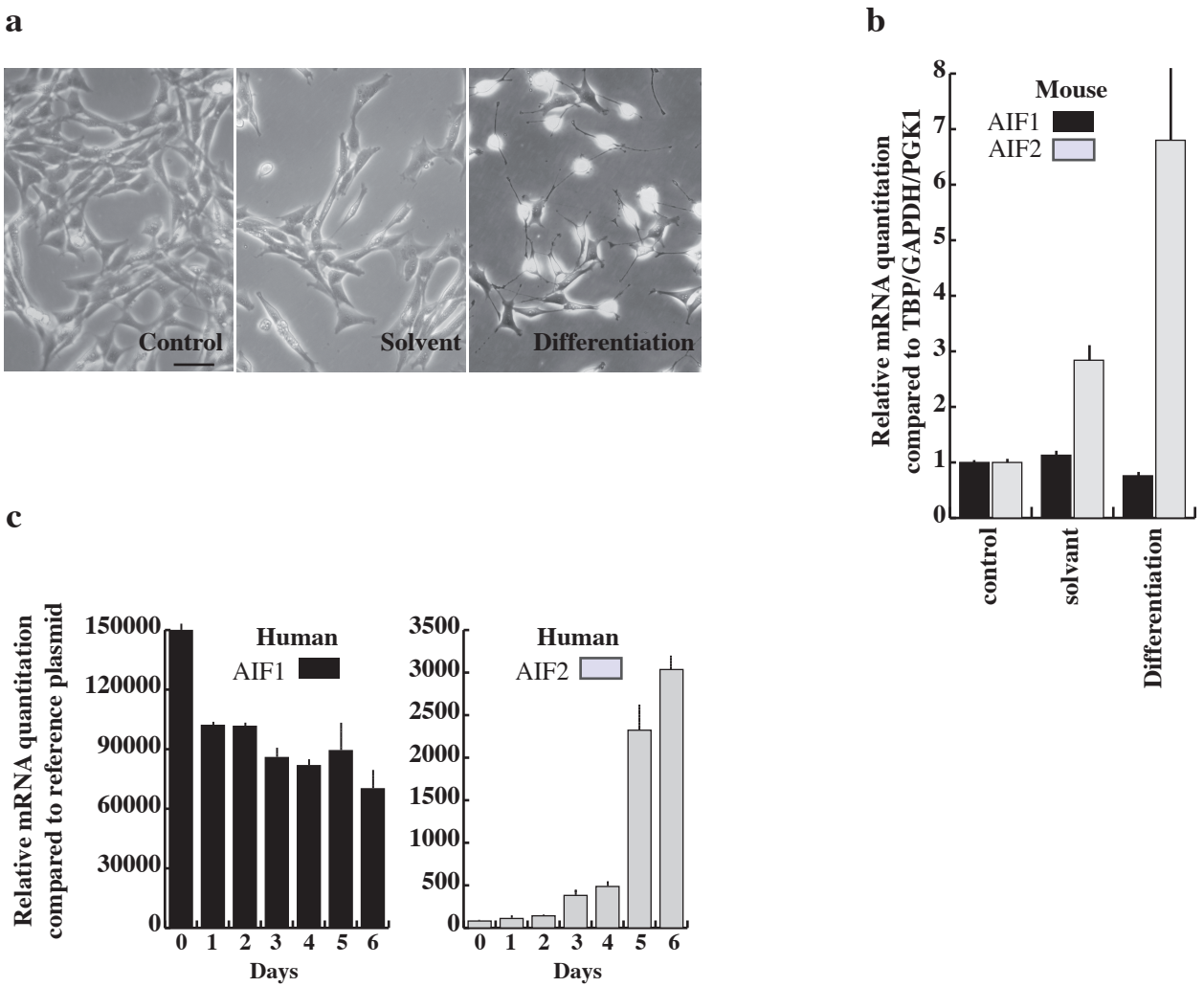

Figure 3

Hangen et al

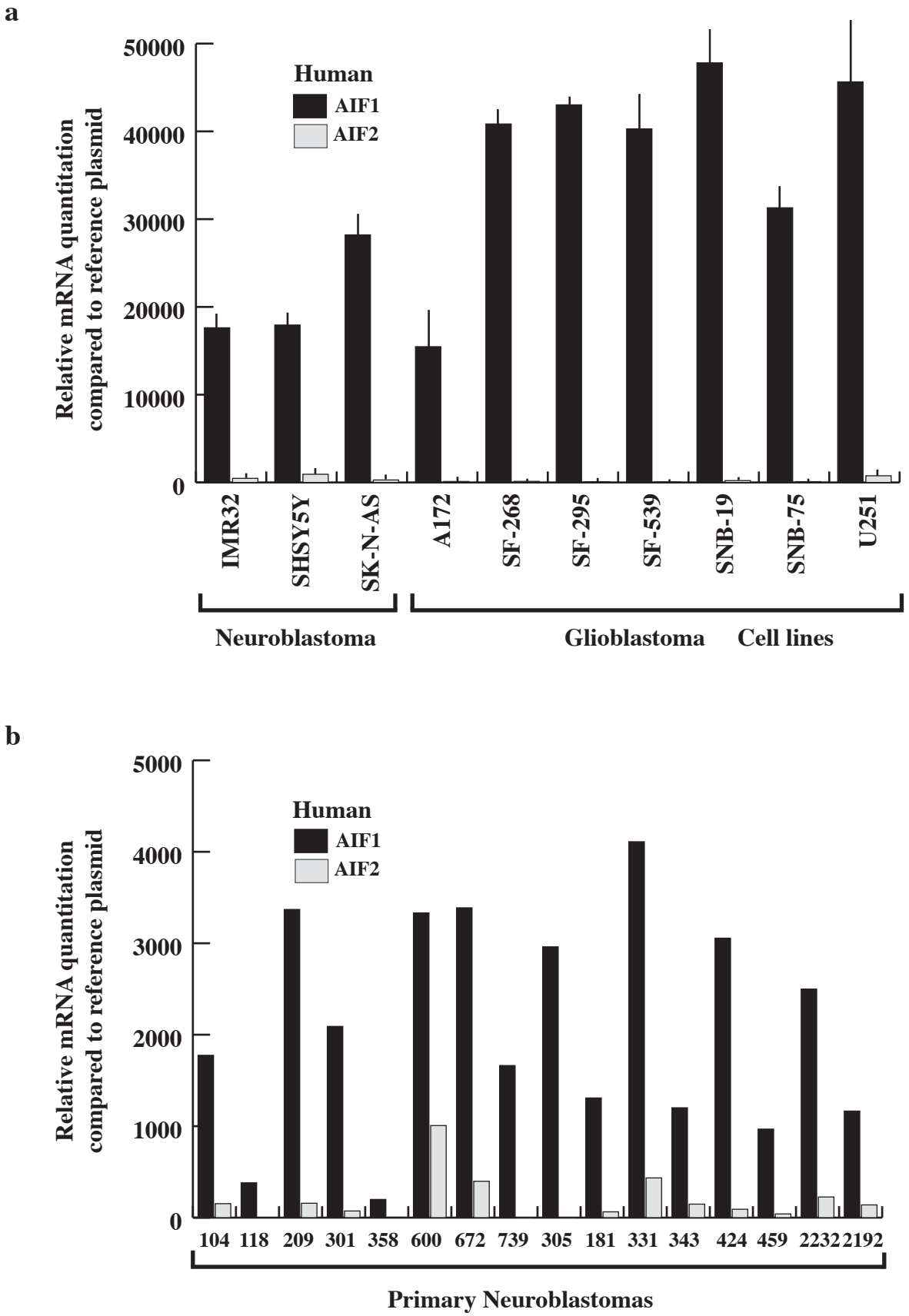

Figure 4
Hangen et al.

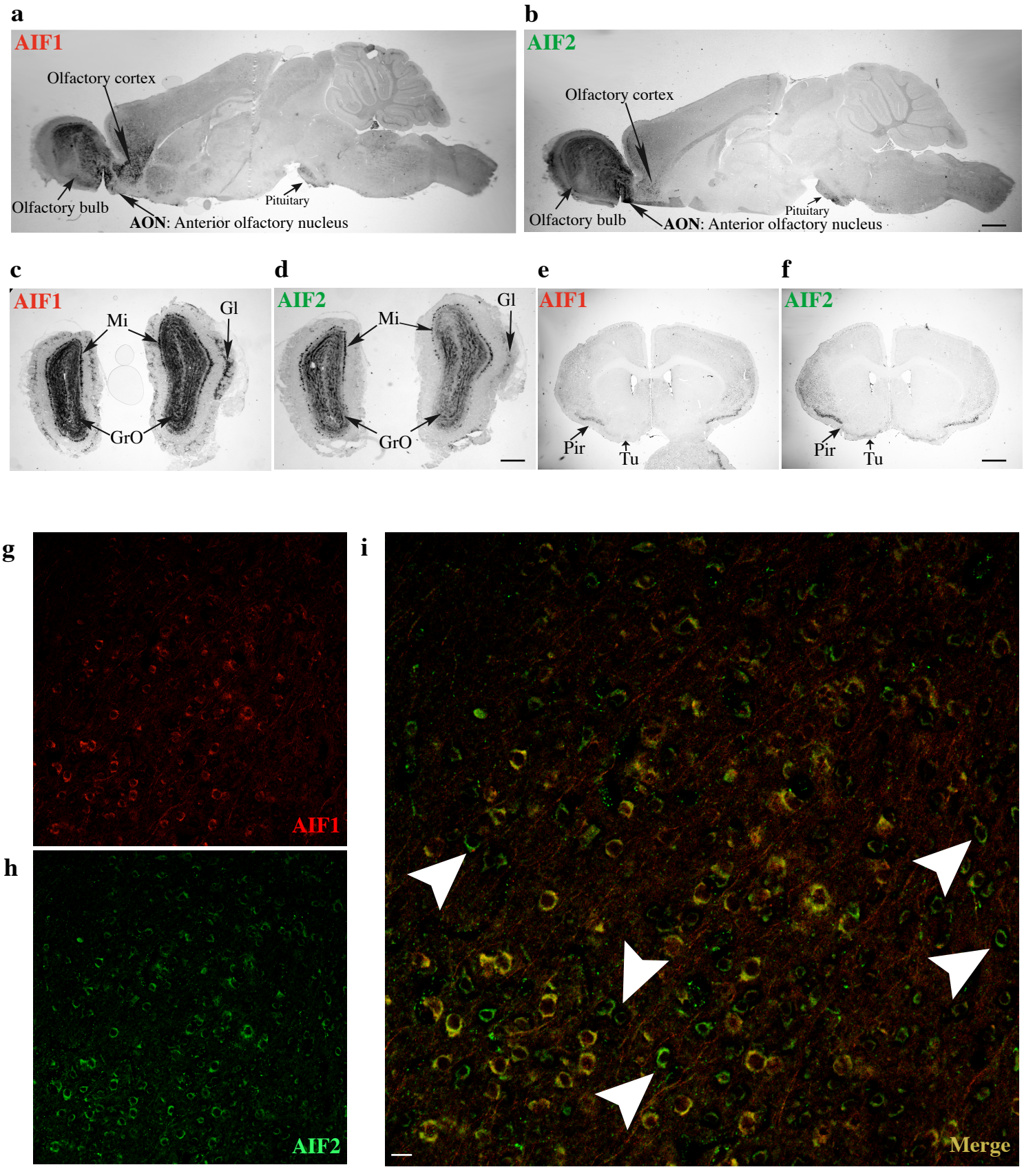

Figure 5

Hangen et al

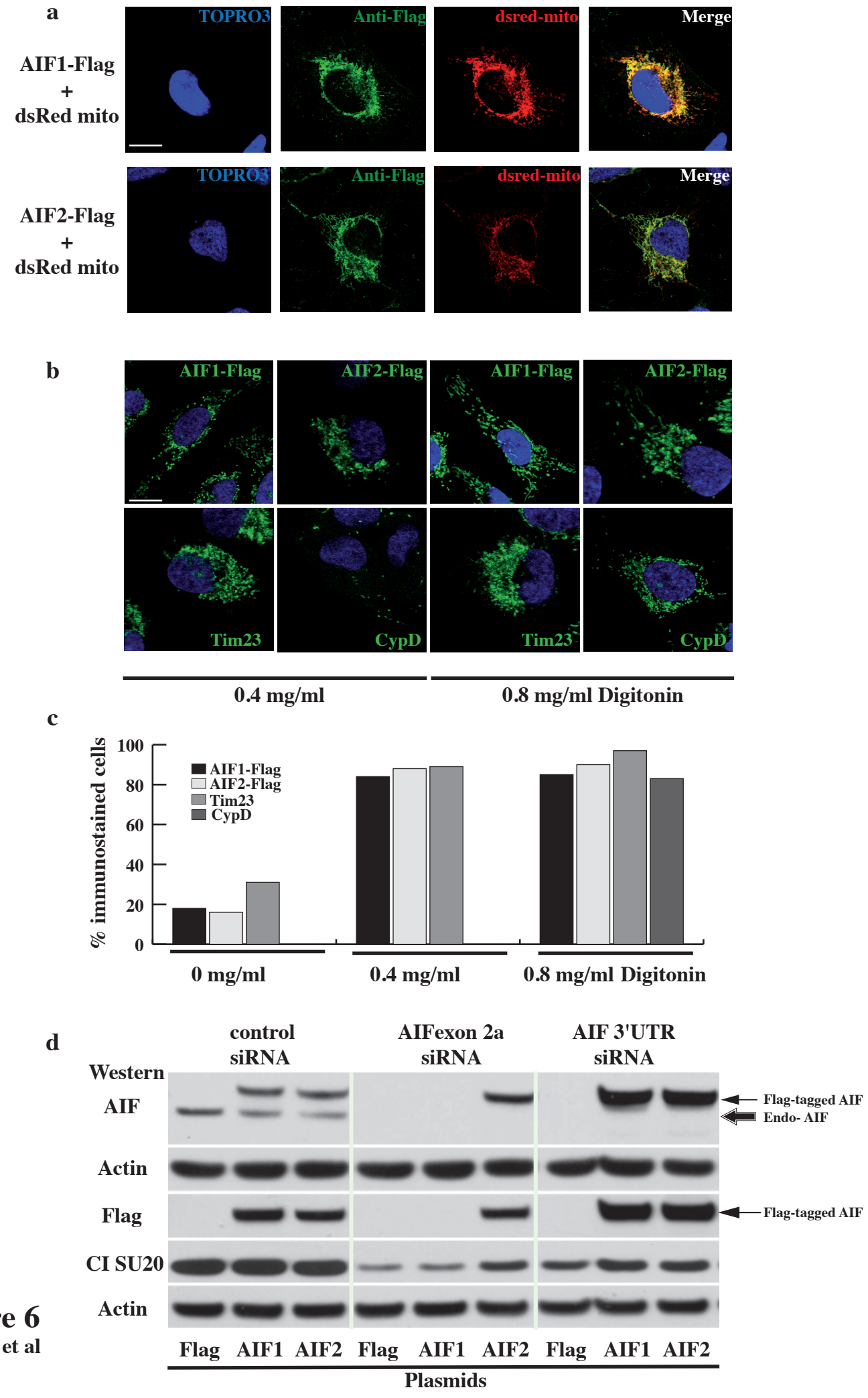

Figure 6
Hangen et al

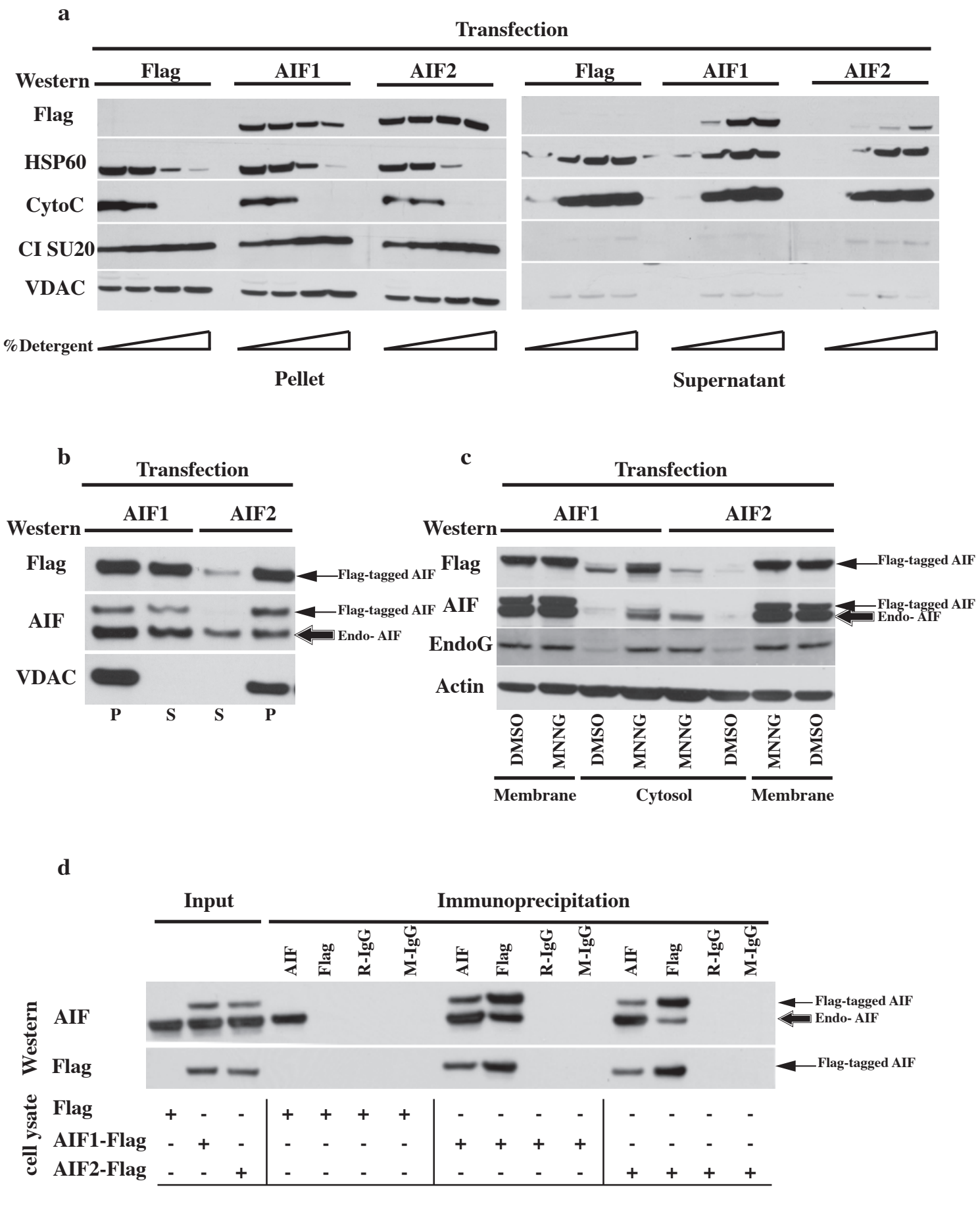

Figure 7
Hangen et al.

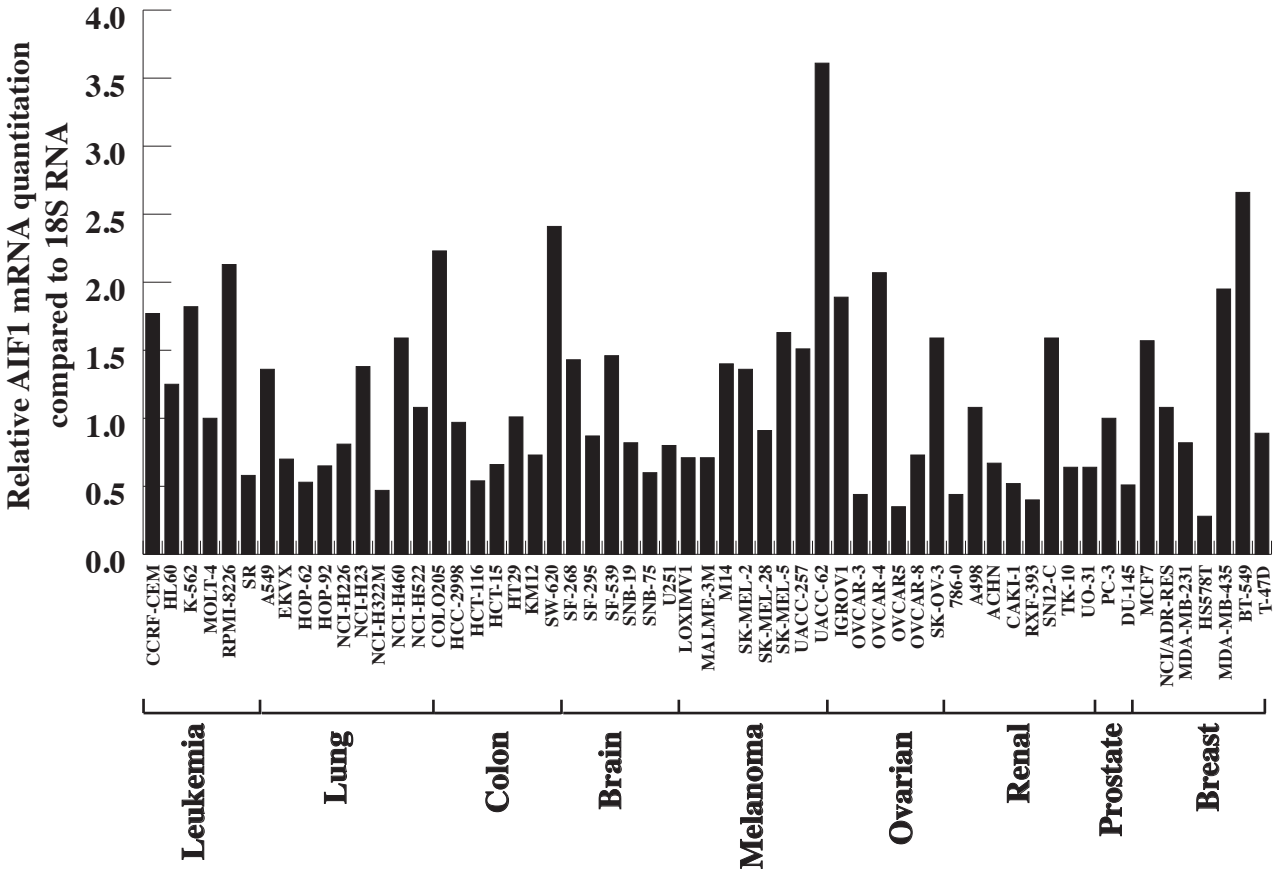

Figure 1 supplemental

Hangen et al

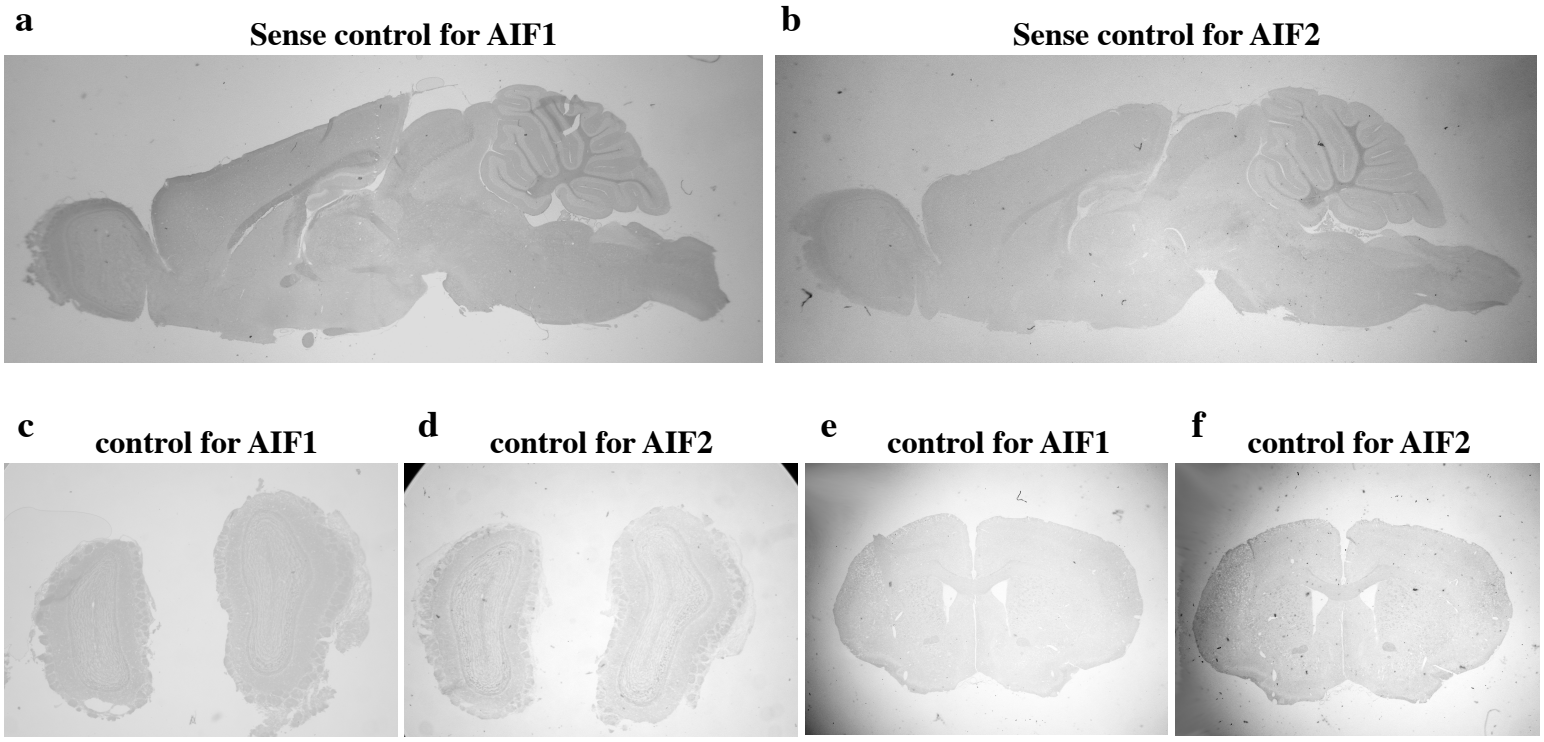

Figure 2 supplemental

Hangen et al.

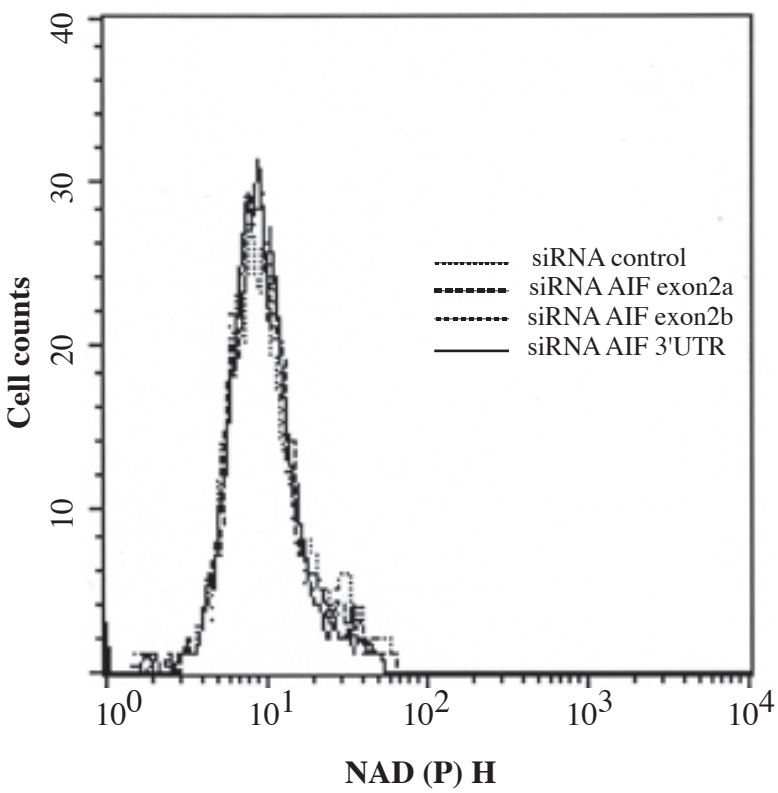

Figure 3 supplemental

Hangen et al.

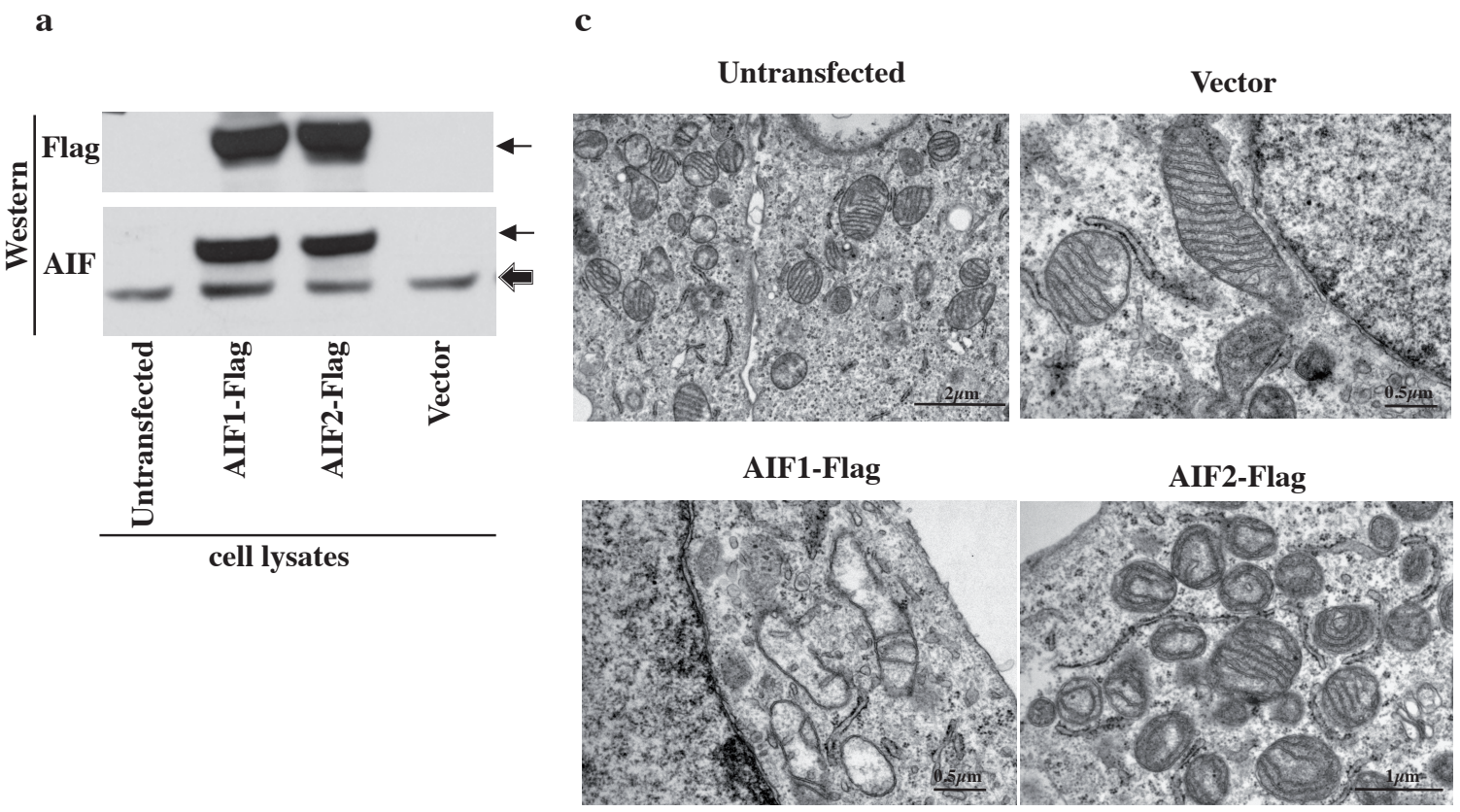

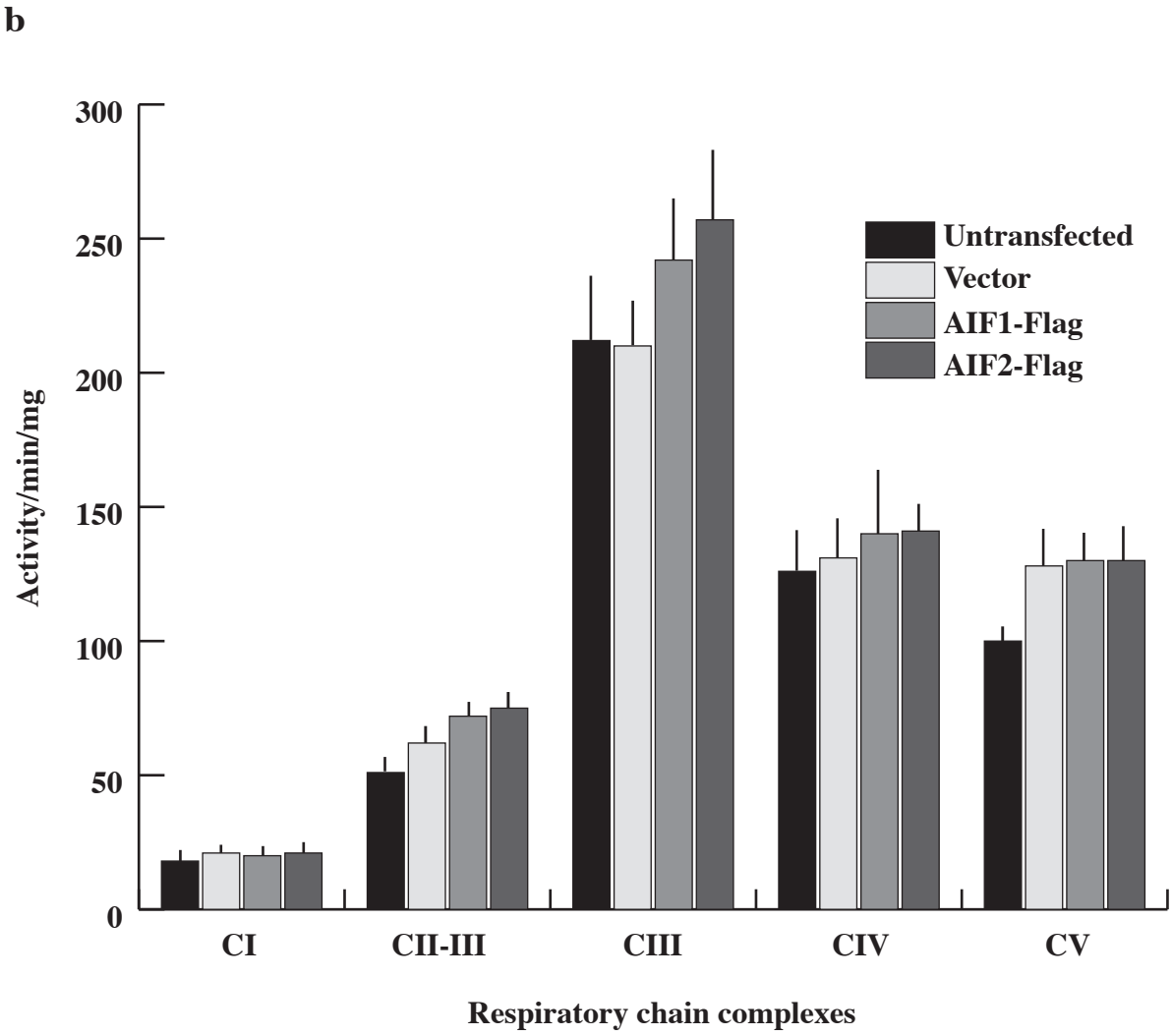

Figure 4 supplemental
Hangen et al.